NASA TECHNICAL NOTE

NASA TN D-6489

c.1

NASA TN D-6489

DYNAMICS OF HIGH-DRAG PROBE SHAPES AT TRANSONIC SPEEDS

by Robert I. Sammonds

Ames Research Center
Moffett Field, Calif. 94035

NATIONAL AERONAUTICS AND SPACE ADMINISTRATION • WASHINGTON, D. C. • SEPTEMBER 1971

1. Report No. NASA TN D-6489	2. Government Accession No.	3. Recipient's Catalog No.
4. Title and Subtitle DYNAMICS OF HIGH–DRAG PROBE SHAPES AT TRANSONIC SPEEDS*		5. Report Date September 1971
		6. Performing Organization Code A-3613
7. Author(s) Robert I. Sammonds		8. Performing Organization Report No.
		10. Work Unit No. 124-07-13-10-00-21
9. Performing Organization Name and Address NASA Ames Research Center Moffett Field, Calif. 94035		11. Contract or Grant No.
		13. Type of Report and Period Covered Technical Note
12. Sponsoring Agency Name and Address National Aeronautics and Space Administration Washington, D.C. 20546		14. Sponsoring Agency Code

15. Supplementary Notes

*The basic results of this investigation were previously reported in AIAA paper 70-564 entitled "Transonic Static- and Dynamic-Stability Characteristics of Two Large-Angle Spherically Blunted High Drag Cones."

16. Abstract

The transonic aerodynamics of spherically blunted 55° and 60° half-angle cones were studied in ballistic-range tests. Both shapes were dynamically unstable at small pitch amplitudes over a small Mach number range near 1.0. The dynamic instability was reduced by moving the center of gravity forward and was eliminated entirely by providing a full-diameter spherical segment afterbody that was made concentric with the center of gravity.

Both models and variations thereof were statically stable in all tests.

17. Key Words (Suggested by Author(s)) Large angle spherically blunted cones; Atmospheric entry vehicles; Mars probe-lander configurations; Transonic aerodynamics of large angle blunted cones; Blunt cones; Dynamic stability; Ballistic range tests	18. Distribution Statement Unclassified – Unlimited

19. Security Classif. (of this report)	20. Security Classif. (of this page)	21. No. of Pages	22. Price*
Unclassified	Unclassified	52	$3.00

*For sale by the National Technical Information Service, Springfield, Virginia 22151

SYMBOLS

A	reference area, maximum body cross-sectional area, m^2
C_D	drag coefficient, drag/$q_\infty A$
C_{L_α}	lift-curve slope, per radian
C_{m_α}	pitching-moment-curve slope (based on linear pitching-moment curve), per radian
$C_{m_q} + C_{m_{\dot\alpha}}$	damping-in-pitch derivative, $\frac{\partial C_m}{\partial(qd/V)} + \frac{\partial C_m}{\partial(\dot\alpha d/V)}$, per radian
d	reference diameter, maximum body diameter, m
I_x	moment of inertia about the roll axis, kg-m^2
I_y	moment of inertia about transverse axis through center of gravity, kg-m^2
M	Mach number
m	mass of model, kg
q	angular pitching velocity, radians/sec
q_∞	free-stream dynamic pressure, N/m^2
Re	Reynolds number based on free-stream air properties and model reference diameter, d
r	radius of curvature of rounded corners and cone apex, m
V	velocity of the model with respect to the still air, km/sec
x_{cg}	axial distance from model nose to center-of-gravity position, m
x,y,z	earth-fixed axes; also displacements along these axes, m
α	angle of attack (angle, projected onto the xz plane, between model longitudinal axis and the stream direction), deg
α_m	average value of maximum-angle envelope, deg
$\bar\alpha_r$	exact resultant angle of attack, $\tan^{-1}\sqrt{\tan^2\alpha + \tan^2\beta}$, deg
β	angle of sideslip (angle, projected onto the xy plane, between model axis of symmetry and the stream direction, deg
ξ	dynamic-stability parameter, $C_D - C_{L_\alpha} + (C_{m_q} + C_{m_{\dot\alpha}})(d/\sigma)^2$

σ	transverse radius of gyration with respect to the center of gravity of the model, $\sqrt{I_y/m}$, m
ρ	free-stream air density, kg/m^3
$(\dot{\ })$	first derivative with respect to time

Subscripts

a	afterbody
b	base
c	corner
f	final
i	initial
l	linear
n	nose
w	wake
∞	free-stream conditions

DYNAMICS OF HIGH–DRAG PROBE SHAPES AT TRANSONIC SPEEDS*

Robert I. Sammonds

Ames Research Center

SUMMARY

The transonic aerodynamics of spherically blunted 55° and 60° half-angle cones were studied in ballistic-range tests. Both shapes were dynamically unstable at small pitch amplitudes over a small Mach number range near 1.0. The dynamic instability was reduced by moving the center of gravity forward and was eliminated entirely by providing a full-diameter spherical segment afterbody that was made concentric with the center of gravity.

Both models and variations thereof were statically stable in all tests.

INTRODUCTION

Experiments proposed for the planet Mars include both the determination of the atmospheric structure and composition through the use of unmanned probes and the landing of instrument packages on the planet's surface (refs. 1-5). One such experiment would determine the structure and mean molecular weight of the atmosphere during entry by on-board measurements of pressure, temperature, and acceleration in appropriate phases of the entry, and would determine atmospheric composition by use of a mass spectrometer.

These objectives require that the vehicle have the following qualities:

1. Known and well-defined motion-response characteristics (aerodynamics) for proper interpretation of the accelerometer measurements.
2. Aerodynamic stability to ensure the proper orientation of the heat shield and instrumentation and for the deployment of a drag device.
3. A low ballistic coefficient to maximize postblackout communication time and to decelerate to speeds at which on-board measurements of temperature and pressure may be made, or speeds at which drag devices may be deployed.

The aerodynamic characteristics of several candidate configurations (large-angle blunted cones) have been determined experimentally throughout a Mach number range from subsonic to hypersonic (refs. 6 and 7) and have been found to be generally favorable except in the transonic-speed range, where potentially serious dynamic instability was observed. The purpose of this study is to investigate the transonic aerodynamic characteristics of two particular

---

*The basic results of this investigation were previously reported in AIAA paper 70-564 entitled "Transonic Static- and Dynamic-Stability Characteristics of Two Large-Angle Spherically Blunted High Drag Cones."

configurations in much greater depth than has previously been attempted. Included are the effects of Mach number, angle of attack, center-of-gravity location, wall interference, Reynolds number, and certain geometry changes.

MODELS

Two configurations were tested, a 55° half-angle blunted cone with a nose-to-base-radius ratio (r_n/r_b) of 1.0 and a 60° half-angle blunted cone with $r_n/r_b = 0.2$. The 60° half-angle cone was tested with and without corner radii (r_c), with two center-of-gravity locations, and two afterbody shapes (flat and spherical). A few tests were made with a 30° half-angle blunted cone afterbody added to the 55° cone.

Pertinent dimensions of these configurations are given in figure 1. The model geometries are also tabulated in table 1. Materials were selected to give the desired mass and center-of-gravity location. These materials were steel, aluminum, tungsten alloy, and polyethylene. The models and sabots are shown in figure 2.

TESTS

The models were tested in free flight, in still air, in both the Ames Pressurized Ballistic Range (PBR) and the Ames Hypervelocity Free-Flight Aerodynamic Facility (Aero) in the transonic speed regime ($M_\infty = 0.4$ to 1.8). Reynolds numbers of the tests, based on model diameter, varied from 100,000 to 400,000. Table 1 summarizes the test conditions and table 2 lists the complete results of the tests.

Model Launching

The models were fired from various smooth-bore guns using both compressed air and gun powder as the energy source. The models were adapted to the guns by means of either two- or four-piece plastic sabots.

Instrumentation

Shadowgraphs of the models were obtained in orthogonal planes at 24 observation stations over a ballistic flight of 62 m (PBR), or at 16 observation stations for a ballistic flight of 23 m (Aero). The photographic observation stations for each facility contain accurately calibrated fiducial systems so that the spatial position and attitude of the model at each station can be determined accurately over the entire length of the flight. Electronic chronographs measured the time of the model flight between stations.

Accuracy of Data

The accuracies of the measured quantities for obtaining the aerodynamic coefficients from the model motions are as follows:

Measurement	PBR	Aero
x,y,z	±0.013 cm	±0.013 cm
α,β	±0.125°	±0.250°
t	0.625 μsec	0.02 μsec
p_∞	0.1 mm Hg	0.1 mm Hg

Reduction of Data

To determine the aerodynamic characteristics of each configuration, their free-flight motions were analyzed by use of the Ames Hypersonic Free-Flight Branch data-reduction program. This program, described in detail in reference 8, determines drag from the time-distance history of each flight, static and dynamic stability from the oscillatory history of the model, and lift-curve slope from the swerve measurements of the model in conjunction with the oscillatory motion.

A typical history of the model motion in the Pressurized Ballistic Range is shown in figure 3. This figure is a plot of α versus β and $\overline{\alpha}_r$ versus distance for the 60° cone at an average Mach number of 1.01. Because of the significant effects of small changes in Mach number and pitching amplitude on dynamic behavior in this speed regime (to be shown in the data), the data reduction was performed on short segments of each model trajectory consisting of three consecutive peaks. In this manner, four to six data points were obtained from each model flight with minimum changes in Mach number and amplitude within each segment analyzed.

RESULTS AND DISCUSSION

The dynamic-stability data in figures 4 and 5 show configurations A, B, and C to be dynamically unstable in the transonic Mach number range. The instability varies with Mach number and pitching amplitude. The dynamic stability of these configurations is neutral in the subsonic speed range, unstable in the Mach number range from 1.0 to 1.4, and neutral again at higher speeds. Constant Mach number crossplots of these data as a function of the pitching amplitude (fig. 6) show that the instability is maximum at the lowest angle of attack, decreasing with increasing amplitude of the oscillation until it reaches a limit cycle of about 20°.

The static-stability coefficients (C_{m_α}) obtained for these two configurations, with reference to the center of volume, are presented in figures 7(a) and (b). These data show both models to be statically stable throughout the Mach number and pitch amplitude ranges of these tests. For the 60° cone (fig. 7(b)), very little change is evident in the static stability with either Mach number or pitch amplitude. For the 55° cone (fig. 7(a)), there was more spread in the data, but it does not appear to correlate with either Mach number or pitching amplitude.

The lift-curve slope C_{L_α} (fig. 8) was essentially the same for both the 60° and 55° cones and varied from approximately -1.1 at Mach numbers greater than 1 to about -0.6 at a Mach number of 0.6. The rate of change of the lift-curve slope between these two points was rather abrupt, occurring near M = 1.

The drag coefficients obtained (fig. 9) show small scatter and define smooth curves, with little effect of pitching amplitudes to about 20°.

Drag coefficients determined from tests in the Ames 2- by 2-Foot Transonic Wind Tunnel (ref. 9) for the 60° cone are compared in figure 9(b) with the results of free-flight tests. These drag data agree remarkably well except at a Mach number of 1.0 where the wind tunnel value was about 10 percent lower than that for free flight. The reason for this discrepancy is not definite, but is thought to be the result of sting and wall interference.

Wall Interference

The aerodynamic characteristics presented for the two cones were obtained from tests in two facilities of quite different dimensions. Because of the possibility of wall interference in the transonic speed range, these differences were useful for assessing interference effects. A series of tests, outlined in table 3, was made to evaluate interference with variations in model scale, Reynolds number, and blockage factor. The results of these tests, summarized in figures 10 to 13 for nominal Mach numbers of 0.95, 1.05, and 1.15, show the following variations:

(1) At a nominal Mach number of 1.05, where the dynamic instabilities previously encountered were large, figure 10 shows that for pitching amplitudes above 12° there is good agreement in the data regardless of the facility or the blockage factor. Below 12°, there appears to be a small effect of facility and Reynolds number but it should be noted that these data are limited. Although the data for the other two Mach numbers are limited, they show similar trends to those observed at M = 1.05.

(2) The static-stability data obtained in the PBR at a Mach number of 1.05 were significantly lower than those obtained in the Aero facility for equal Reynolds numbers and blockage factors, especially for the smaller pitching amplitudes (fig. 11). At Mach numbers of 0.95 and 1.15 this effect of facility on the static stability tends to diminish. In the Aero facility, increasing the blockage factor from 0.03 to 0.19 percent had little or no effect on the stability at a Mach number of 1.05, but increased the stability at the higher Mach number (one data point). In addition, decreasing the Reynolds number for a constant blockage factor had little effect on the static stability. In the PBR, however, simultaneously decreasing the Reynolds number and the blockage factor significantly increased the stability of the model at all three Mach numbers, particularly at M = 1.05.

(3) The lift-curve slope (fig. 12) was not significantly affected by either Reynolds number, blockage factor, or facility at any of the Mach numbers shown.

(4) Drag coefficients obtained in the Aero facility were approximately 5 percent lower than those obtained in the PBR for constant Reynolds number and blockage factor (fig. 13(a)). Reducing the Reynolds number from 0.23 to 0.08×10^6 in the Aero facility increased the drag by about

5 percent when the blockage factors were held constant (fig. 13(b)). Increasing the blockage factor from 0.03 to 0.19 percent, however, reduced the drag coefficient from 1.23 to 1.14 at M = 1.04, but above M = 1.15, this effect of blockage disappears (fig. 13(c)). Decreasing the blockage factor from 0.03 to 0.004 percent while simultaneously changing from the Aero facility to the PBR (fig. 13(d)) and keeping the Reynolds number essentially constant caused an increase in the drag coefficient comparable to the increase noted in figure 13(a) when only the facility was varied. This suggests that the variation in the blockage factor from 0.03 to 0.004 percent did not significantly affect the drag of the model.

Briefly, these results show that: (1) changing from the Aero facility to the PBR significantly reduced the static stability of the model and increased the drag coefficient by 5 percent but had no appreciable effect on either the dynamic stability or the lift-curve slope; (2) varying the Reynolds number had no consistent effect on the dynamic stability, lift-curve slope or static stability obtained in the Aero facility, but changed the drag coefficient by 5 percent; (3) varying the blockage factor from 0.03 to 0.19 percent significantly affected the drag coefficient at $M_\infty = 1.04$ but had little or no effect on the dynamic stability, static stability, or lift-curve slope; (4) decreasing the blockage factor by an order of magnitude (0.03 to 0.004 percent) for a constant Reynolds number significantly increased the static stability of the model but had little or no effect on the dynamic stability, lift-curve slope, or drag coefficient.

These results lead to the conclusion that interference effects are experienced at blockage factors above 0.03 percent and for tests in the PBR. However, these interference effects manifest themselves mainly by affecting the drag coefficient and the static stability. Interference effects on the dynamic stability are either insignificant or at least within the accuracy of the data.

The basic data for these tests are presented in appendix A.

Because the mechanism of the blockage or interference effects is not understood, a brief description of the facilities used may be enlightening.

Model A was tested in the Hypervelocity Free-Flight Aerodynamic Facility (fig. 14). This facility, shown on the left, is octagonal in cross section, has smooth solid walls, and has all of its electronics, optics and fiducial system located on the outside of the tunnel structure. The test section itself is tapered in the direction of the model flight to accommodate the boundary-layer growth when the facility is used with a counterflow airstream.

Model B, on the other hand, was tested in the PBR. This facility, shown on the right of figure 14, consists of a shell, circular in cross section, having the film platens, spark light sources, fiducial system and photobeams inside the range shell. It is difficult to show all the pertinent details of the interior of this facility in one photograph. However, the uprange photograph on the right shows the film platens, blast shields and the station structure but not the 3.04-m shell that encloses it. The distance from the range centerline to the film platen increases as the model travels downrange as indicated by the dimensions given for the various stations. Since each film platen is only 0.5 m wide, the time or distance that the model is adjacent to the film station is about 20 percent of that required for the entire flight. In other words, for about 80 percent of the model's flight the only parts of the range structure that could influence the model are the range shell itself and the floor of the range. It should also be noted that the station spacing is not uniform but varies from 2.1 m to as much as 4.2 m.

Modifications of Basic Models

As a direct result of the instabilities determined for the two configurations, a few tests were conducted with the objective of either eliminating the instabilities or understanding them better. The following geometric modifications were thus made to the original 60° half-angle blunted cone for the reasons stated:

(1) The corner was made sharp (model E, fig. 1) to investigate the effect of rounding on the dynamic instability.

(2) The center of gravity was moved 6 percent forward of that for the basic configuration (see table 1) to determine the variation of dynamic stability as a function of the center of gravity.

(3) A spherical segment afterbody was added to the original configuration, the center of curvature of which was at the center of gravity of the model. This center of gravity location was held at the same position as that for the basic configuration (model F, fig. 1 and table 1) in an attempt to identify the part of the body that contributes the destabilizing dynamic moments. Note that a spherical afterbody with its center of curvature at the center of gravity cannot produce moments about the center of gravity due to pressure forces, since all pressure forces act through the center of gravity.

Eliminating the corner radius (fixing the separation point) had essentially no effect on the aerodynamic behavior of the blunted 60° cone (model E) except that the drag was increased by about 10 percent at all speeds (figs. 15(e) and 16).

Moving the center of gravity of model C forward from $x_{cg}/d = 0.23$ to 0.17 decreased the tendency of the model oscillation to diverge and reduced the limit cycle amplitude as well (fig. 17). The damping comparison is shown best in figure 18 for a Mach number of 1.05. Damping coefficients determined from Jet Propulsion Laboratory free-flight tests in the Ames 6- by 6-Foot Wind Tunnel by the method of reference 8 agree well with the ballistic-range data (fig. 18).

Adding the full-diameter spherical segment afterbody to model C completely eliminated the dynamic instabilities previously encountered with the flat base (figs. 19 and 20). Note that even the oscillation of 1.9° amplitude is, at worst, neutrally stable at $M_\infty = 1.0$. Since this afterbody was intended to eliminate the moment contribution caused by pressure forces acting on the base, it is concluded that irregular pressures on the flat base are highly destabilizing. The flight speed and local airspeeds in the flow field, however, are subsonic and transonic so that the afterbody could also affect the pressures on the front face. The slight reduction in drag coefficient and decrease in static stability due to the spherical afterbody (figs. 21 and 22) may be evidence of the influence of the afterbody on the forebody flow field, but they could also be a direct result of afterbody pressures. The lift-curve slopes were unaffected by afterbody shape.

Shadowgraph pictures of the two models at comparable Mach numbers and angles of attack are presented in figure 23. These pictures show that model F had the narrower wake and further extending shock waves in the vicinity of the shoulder. Thus, the flow pictures show evidence of changes in the aerodynamic properties, demonstrated in detail by the drag coefficient and pitching moment. Some wake diameter measurements are compared in table 4.

CONCLUSIONS

The transonic aerodynamic characteristics of two Mars probe-lander candidates have been determined experimentally in free flight in still air. These data indicate the following:

1. The two basic shapes tested (60° and 55° half-angle blunted cones) have similar regions of dynamic instability in the transonic-speed range. The dynamic stability is neutral in the subsonic-speed range, unstable at Mach numbers from 1.0 to 1.4, and neutral at higher speeds. The degree of instability varies with pitching amplitude, being greatest at small amplitudes and approaching neutral stability (limit cycle) at about 20°.
2. Modifications in afterbody geometry are capable of eliminating the transonic dynamic instability. In particular, a full diameter spherical segment afterbody with its center of curvature at the center of gravity yields a dynamically stable configuration.
3. Eliminating the corner radius of the 60° cone had no significant effect on the dynamic behavior of the model. However, moving the center of gravity location forward reduced both the instability and the apparent limit cycle amplitude.
4. The transonic drag coefficients of the round-cornered 60° cone were approximately 10 percent lower than those of the sharp-cornered 60° cone over the entire Mach number range of these tests (0.6–1.8).
5. Interference effects on the dynamic stability and lift-curve slope of model C were either insignificant or at least within the accuracy of the data. However, moderate variations in the static stability and drag, apparently due to wall and equipment interference, were encountered at blockage factors above 0.03 percent and for the tests made in the PBR.
6. All configurations were statically stable and had negative lift-curve slopes.

Ames Research Center
National Aeronautics and Space Administration
Moffett Field, Calif., 94035, June 10, 1971.

APPENDIX A

BASIC DATA FOR WALL INTERFERENCE TESTS

The complete set of data used for the comparison plots in figures 10 to 13 are presented in figures 24 to 26. These data show the variation of dynamic and static stability, lift-curve slope, and drag coefficient as a function of Mach number for Reynolds numbers of approximately 0.1×10^6 and 0.2×10^6 and blockage factors of 0.03 and 0.19 percent in the Aerodynamic facility and for a blockage factor of 0.004 percent in the PBR.

REFERENCES

1. Seiff, Alvin; and Reese, David E., Jr.: Defining Mars' Atmosphere – A Goal for Early Missions. Astronaut. Aeronaut., vol. 3, no. 2, Feb. 1965, pp. 16-21.

2. Roberts, Leonard: Entry Into Planetary Atmospheres. Astronaut. Aeronaut., vol. 2, no. 10, Oct. 1964, pp. 22-29.

3. Martin, J.S., Jr.; Bowen, F.W., Jr.; et al.: 1973 Viking Voyage to Mars. Astronaut. Aeronaut., vol. 7, no. 11, Nov. 1969, pp. 30-58.

4. Sommer, Simon C.; Boissevain, Alfred G.; Yee, Layton; and Hedlund, Roger C.: The Structure of an Atmosphere from On-Board Measurements of Pressure, Temperature, and Acceleration. NASA TN D-3933, 1967.

5. Peterson, Victor L.: A Technique for Determining Planetary Atmosphere Structures from Measured Accelerations of an Entry Vehicle. NASA TN D-2669, 1965.

6. Sammonds Robert I.: Aerodynamics of Mars Entry Probe-Lander Configurations at a Mach number of 10. NASA TN D-5608, 1970.

7. Krumins, Margonis V.: Drag and Stability of Mars Probe/Lander Shapes. J. Spacecraft Rockets, vol. 4, no. 8, Aug. 1967, pp. 1052-1057.

8. Malcolm, Gerald N.; and Chapman, Gary T.: A Computer Program for Systematically Analyzing Free-Flight Data to Determine the Aerodynamics of Axisymmetric Bodies. NASA TN D-4766, 1968.

9. Marko, Wayne J.: Static Aerodynamic Characteristics of Three Blunted Sixty-Degree Half-Angle Cones at Mach Numbers from 0.60 to 1.30. TR 32-1298, Jet Propulsion Laboratory, Pasadena, Calif., July 1, 1968.

TABLE 1.- SUMMARY OF MODEL CONFIGURATIONS AND AVERAGE TEST CONDITIONS

Model	Cone half-angle	r_n/r_b	r_c/r_b	x_{cg}/d from nose	Diameter, cm	$I_y \times 10^{-3}$, g-cm^2	I_y/I_x	$\rho_\infty \times 10^3$, g/cm^3	M_∞	$Re \times 10^{-6}$, diam	α_m, deg	md^2/I_y	After-body	Facility
A	55°	1.0	0	0.17	2.032	0.0023	0.549	0.345	0.89-1.14	0.12-0.15	4-25	23.4	Flat	Aero[1]
B	↓	↓	↓	0.20	↓	0.0015	0.654	0.110	0.66-0.84	0.28-0.36	16-23	20.6	Conical[2]	↓
C	60°	0.2	0.1	0.23	5.080	0.12	0.544	0.24-0.29	0.6-1.8	0.17-0.46	4-20	21.5	Flat	PBR[3]
C	↓	↓	↓	↓	↓	0.043	0.545	0.248	0.6-1.4	0.15-0.31	12-35	21.4	↓	Aero
C					2.032	0.0013-0.0028	0.552	0.20-0.60	0.8-1.21	0.08-0.26	6-28	21.3		Aero
C					↓	0.0027	0.550	0.118	0.8-1.4	0.04-0.06	7-16	21.5		PBR
D				0.17	5.080	0.067	0.582	0.146	0.8-1.65	0.15-0.22	5-38	29.2		↓
E			0	0.27	↓	0.089	0.576	0.283	0.7-1.52	0.20-0.35	6-18	25.9		
F			0.1	0.23		0.18	0.731	0.352	0.98-1.41	0.34-0.46	2-10	19.8	Spherical[4]	

[1]Aerodynamic Hypervelocity Free-Flight Facility.
[2]30° half-angle cone with bluntness ratio (r_a/r_b) of 0.25, base radius = 0.555 r_b (forebody base radius).
[3]Pressurized Ballistic Range.
[4]Center of curvature of full diameter spherical afterbody located at center of gravity of model.

TABLE 2.- DATA SUMMARY FOR THE TWO BASIC CONFIGURATIONS.

(a) Pressurized Ballistic Range

Model C; $\theta_c = 60°$; $x_{cg}/d = 0.23$; $d \approx 5.080$ cm

Run	Sta. Int.	C_D	$-C_{m_\alpha}$, per rad	C_{L_α}, per rad	ξ	$C_{m_q} + C_{m_{\dot\alpha}}$	M_∞	$Re\times10^{-6}$	$\rho_\infty\times10^3$, g/cm^3	α_{rms}, deg	α_m, deg	α_m/α_{min}	α,β dev., deg	y,z dev., cm	d, cm	$m\times10^{-3}$, g	$I_y\times10^{-3}$, g-cm^2	I_y/I_x	md^2/I_y	$\rho_\infty A/2m\times10^4$, cm^{-1}
983	4-14	1.251	0.145	-0.782	22.284	0.947	1.05	0.2378	0.2358	2.88	4.18	139.4	0.198	0.0226	5.0800	0.1014	0.1223	0.5443	21.394	0.2357
	7-18	1.259	.140	-1.112	18.457	.752	1.03	.2322		3.29	5.05	36.1	.224	.0389						
	10-20	1.224	.135	-1.066	16.599	.669	1.00	.2265		4.30	6.01	60.1	.219	.0389						
	13-23	1.179	.133	-.904	11.242	.428	.98	.2211		4.66	6.97	99.8	.221	.0114						
984	3-13	1.256	.133	-1.002	12.418	.478	1.08	.2505	.2423	6.09	7.56	1.8	.186	.0190	5.0775		.1222	.5436	21.391	.2418
	7-17	1.270	.128	-1.111	10.897	.398	1.05	.2441		6.84	8.42	1.9	.208	.0132						
	9-20	1.270	.127	-1.103	5.729	.157	1.02	.2378		7.26	8.83	1.7	.300	.0147						
	12-22	1.238	.129	-.987	3.073	.040	1.00	.2324		7.62	9.14	1.7	.114	.0198						
	16-24	1.163	.124	-.901	.889	-.055	.98	.2274		7.63	9.24	1.6	.132	.0129						
987	4-14	1.290	.132	-1.067	10.467	.380	1.14	.2761	.2495	6.41	7.83	1.6	.177	.0165	5.0800	.1015	.1225	.5454	21.370	.2492
	7-18	1.279	.129	-1.062	10.765	.394	1.11	.2692		7.12	8.54	1.5	.228	.0144						
	10-21	1.287	.127	-1.090	9.738	.345	1.08	.2606		7.89	9.42	1.5	.290	.0178						
	14-24	1.281	.128	-1.120	7.211	.225	1.05	.2528		8.64	10.19	1.4	.261	.0358						
989	4-13	1.261	.138	-.981	17.556	.715	1.06	.2952	.2887	4.95	6.23	1.7	.283	.0124	5.0775	.1013	.1219	.5436	21.426	.2884
	7-16	1.259	.138	-.988	12.441	.476	1.03	.2884		5.68	6.96	1.6	.214	.0173						
	9-19	1.218	.133	-.975	7.599	.252	1.01	.2803		6.33	7.75	1.6	.272	.0203						
	12-22	1.150	.129	-.876	3.710	.079	.98	.2717		6.79	8.48	1.7	.293	.0198						
	15-24	1.094	.129	-.781	2.697	.038	.95	.2661		7.07	8.88	1.8	.260	.0282						
1057	7-17	1.011	.138	-.677	2.270	.027	.90	.2422	.2811	5.17	7.43	6.3	.236	.0208		.1009	.1209	.5447	21.513	.2820
	9-20	.989	.137	-.619	.563	-.049	.88	.2365		5.35	7.66	6.3	.165	.0178						
	12-22	.976	.138	-.621	2.094	.023	.86	.2317		5.46	7.72	5.8	.199	.0300						
	16-24	.952	.139	-.636	2.050	.022	.84	.2270		5.45	7.89	5.8	.180	.0422						
1058	4-13	1.342	.118	-1.158	2.700	.009	1.38	.3742	.2815	9.83	13.39	4.9	.499	.0223	5.0805	.1001	.1199	.5444	21.562	.2850
	7-18	1.334	.117	-1.137	2.623	.007	1.33	.3616		9.61	13.83	5.2	.506	.0180						
	9-20	1.327	.116	-1.126	1.250	-.056	1.30	.3522		9.94	14.51	5.1	.169	.0261						
	13-23	1.306	.116	-1.113	2.985	.026	1.25	.3391		10.44	14.79	4.8	.258	.0140						
	16-24	1.286	.116	-1.124	3.203	.037	1.23	.3331		10.88	15.05	4.4	.431	.0155						
1059	3-12	.994	.132	-.911	-.984	-.134	.87	.2342	.2802	6.82	9.70	11.3	.337	.0216	5.0798		.1197		21.585	.2835
	6-16	.990	.133	-.860	-.908	-.128	.85	.2293		6.60	9.70	15.4	.344	.0246						
	9-19	.967	.133	-.811	-.705	-.115	.83	.2236		6.64	9.61	17.5	.188	.0246						
	11-21	.959	.132	-.794	-1.234	-.138	.81	.2198		6.57	9.55	14.9	.224	.0228						
	15-24	.920	.133	-.700	1.190	-.020	.80	.2146		6.56	9.55	13.7	.227	.0409						
1060	3-13	1.261	.116	-1.075	2.434	.005	1.10	.3008	.2828	12.74	18.69	11.3	.196	.0160	5.0792	.0996	.1188		21.626	.2877
	7-17	1.260	.118	-1.057	1.545	-.036	1.07	.2917		13.13	19.10	9.6	.319	.0239						
	9-20	1.262	.121	-1.085	2.074	-.013	1.04	.2828		13.03	19.43	9.9	.369	.0221						
	12-22	1.239	.122	-1.048	3.476	.055	1.01	.2753		13.78	20.00	9.1	.282	.0315						
	16-24	1.165	.123	-1.003	2.161	.000	.98	.2682		14.21	20.28	8.9	.297	.0211						
1061	4-13	.896	.136	-.739	3.084	.067	.66	.1775	.2810	3.12	4.49	7.0	.159	.0290	5.0800	.1004	.1205		21.504	.2838
	7-17	.886	.134	-.678	3.414	.086	.65	.1742		3.25	4.70	8.1	.216	.0419						
	9-19	.882	.131	-.686	3.632	.096	.63	.1712		3.43	4.93	7.4	.208	.0632						
	12-22	.897	.130	-.587	1.251	-.011	.62	.1673		3.52	5.12	9.0	.219	.0429						
	16-24	.888	.132	-.372	1.233	-.001	.61	.1642		3.63	5.16	11.2	.107	.0569						
1117	3-13	1.311	.140	-1.140	13.544	.514	1.27	.3531	.2862	3.21	4.61	19.2	.370	.0246	5.0749	.0997	.1191		21.559	.2903
	7-17	1.314	.136	-1.173	13.902	.529	1.23	.3418		3.58	5.35	11.1	.219	.0165						
	9-20	1.309	.134	-1.276	11.334	.406	1.19	.3310		4.40	6.35	10.0	.301	.0269						
	12-22	1.301	.125	-1.153	13.225	.499	1.16	.3217		4.96	7.43	7.5	.308	.0259						
	15-24	1.308	.124	-1.162	13.430	.508	1.13	.3141		6.03	8.30	4.8	.342	.0318						
1119	8-18	1.322	.135	-1.118	4.058	.076	1.34	.3727	.2869	8.94	12.36	3.1	.277	.0241	5.0772	.1017	.1225	.5447	21.413	.2855
	10-20	1.318	.134	-1.122	4.199	.082	1.31	.3638		9.82	12.80	2.9	.228	.0157						
	13-22	1.300	.133	-1.118	5.358	.137	1.27	.3545		10.16	13.40	2.8	.244	.0183						
	16-24	1.318	.133	-1.045	5.301	.137	1.24	.3462		10.71	13.98	2.6	.233	.0140						

TABLE 2.- DATA SUMMARY FOR THE TWO BASIC CONFIGURATIONS - Continued.

Run	Sta. Int.	C_D	$-C_{m_\alpha}$, per rad	C_{L_α}, per rad	ξ	$C_{m_q} + C_{m_{\dot\alpha}}$	M_∞	$Re \times 10^{-6}$	$\rho_\infty \times 10^3$, g/cm^3	α_{rms}, deg	α_m, deg	α_m/α_{min}	α,β dev., deg	y,z dev., cm	d, cm	$m \times 10^{-3}$, g	$I_y \times 10^{-3}$, g-cm^2	I_y/I_x	md^2/I_y	$\rho_\infty A/2m \times 10^4$, cm^{-1}
1120	6-16	1.356	0.131	-1.001	15.326	0.601	1.36	0.3773	0.2864	4.98	6.92	3.0	0.657	0.0282	5.0655	0.0989	0.1176	0.5446	21.587	0.2917
	8-19	1.333	.125	-.988	12.605	.476	1.32	.3665		5.80	7.89	2.3	.406	.0280						
	11-22	1.315	.125	-1.019	10.110	.360	1.28	.3532		6.95	8.92	2.0	.392	.0180						
	15-24	1.326	.124	-.993	9.664	.340	1.24	.3432		7.61	9.72	1.8	.275	.0190						
1151	3-13	.822	.126	-.504	.076	-.058	.45	.1254	.2873	11.19	16.60	118.5	.347	.0096	5.0795	.1001	.1202	.5456	21.487	.2907
	7-17	.825	.125	-.520	-2.494	-.179	.44	.1229		11.05	16.39	86.3	.489	.0262						
1154	4-14	1.396	.119	-1.052	2.178	-.013	1.77	.4862	.2857	7.93	11.61	13.7	.120	.0175	5.0754	.0997	.1194	.5454	21.498	.2900
	7-17	1.409		-1.084	2.508	.001	1.72	.4738		8.19	11.78	11.3	.167	.0198						
	9-20	1.403		-1.154	1.740	-.038	1.66	.4575		7.97	11.98	11.0	.260	.0178						
	12-23	1.386		-1.172	2.608	.002	1.60	.4411		8.45	12.39	9.9	.288	.0145						
Model C; θ_c = 60°; x_{cg}/d = 0.23; d ≈ 2.032 cm																				
1263	5-17	.949	.143	-.591	1.817	.013	.82	.03664	.1156	4.95	7.19	11.4	.272	.0145	2.0345	.01452	.002820	.5520	21.322	.1294
	8-20	.947	.142	-.680	.396	-.058	.81	.03624		5.08	7.25	11.7	.315	.0216						
	10-22	.936	.145	-.716	4.536	.135	.81	.03596		5.08	7.29	10.1	.363	.0269						
	13-24	.928	.143	-.709	-3.334	-.233	.80	.03566		5.12	7.41	13.5	.360	.0282						
1265	5-17	.981	.142	-.647	1.537	-.004	.84	.03735	.1153	5.75	8.41	30.0	.320	.0206	2.0307	.01427	.002746	.5524	21.432	.1309
	8-19	.969	.143	-.701	1.621	-.002	.84	.03699		5.94	8.47	22.9	.304	.0226						
	10-22	.964	.143	-.759	5.840	.192	.83	.03662		6.04	8.70	27.2	.286	.0251						
	13-24	.952	.143	-.723	5.950	.200	.82	.03630		6.10	8.84	25.3	.305	.0231						
1285	5-15	1.375	.148	-1.292	.620	-.095	1.37	.06257	.1178	5.90	8.27	6.9	.243	.0147	2.0333	.01412	.002701	.5516	21.616	.1355
	7-18	1.378	.151	-1.355	-4.904	-.353	1.36	.06189		5.59	7.97	6.1	.388	.0173						
	9-20	1.375	.150	-1.289	-4.357	-.325	1.34	.06110		5.60	8.03	5.2	.409	.0168						
	11-22	1.362	.152	-1.269	-.118	-.127	1.33	.06038		5.55	7.94	5.9	.395	.0287						
	13-24	1.353	.151	-1.188	4.388	.086	1.31	.05979		5.82	7.99	5.4	.416	.0305						
1286	5-16	1.262	.151	-1.025	-.232	-.117	1.06	.04888	.1190	6.58	9.56	17.7	.299	.0206	2.0340	.01429	.002752	.5510	21.477	.1354
	7-19	1.261	.152	-1.034	2.969	.031	1.05	.04835		6.81	9.71	12.8	.282	.0198						
	9-21	1.259	.151	-1.012	8.700	.299	1.04	.04779		6.92	10.02	10.5	.374	.0239						
	12-23	1.259	.149	-.972	11.083	.412	1.02	.04718		7.13	10.35	9.5	.302	.0241						
1288	4-16	1.084	.143	-.808	-.423	-.107	.95	.04390	.1192	5.33	7.38	3.2	.365	.1421	2.0320	.01415	.002698	.5481	21.648	.1367
	7-20	1.067	.141	-.832	2.562	.031	.94	.04332		5.51	7.44	3.3	.344	.1270						
	9-21	1.059	.141	-.900	1.890	-.003	.93	.04299		5.39	7.52	3.4	.315	.0206						
	12-23	1.046	.138	-.795	1.417	-.020	.92	.04253		5.44	7.51	3.2	.131	.0213						
1289	5-17	1.317	.137	-1.037	.758	-.075	1.13	.05190	.1185	10.41	15.29	764.0	.208	.0178	2.0345	.01444	.002789	.5478	21.436	.1333
	8-19	1.308	.137	-1.072	.515	-.087	1.12	.05122		10.75	15.33	306.5	.168	.0195						
	10-22	1.302	.137	-1.071	.417	-.091	1.10	.05052		10.56	15.34	191.7	.245	.0213						
	13-24	1.285	.137	-1.080	-1.836	-.196	1.09	.04992		10.53	15.37	219.8	.246	.0221						
1290	5-17	1.123	.142	-.826	3.631	.078	.96	.04333	.1173	10.13	14.84	22.8	.284	.0257	2.0351	.01428	.002751	.5492	21.508	.1336
	7-20	1.086	.142	-.771	3.258	.065	.95	.04289		10.81	15.06	25.1	.264	.0267						
	9-21	1.056	.141	-.766	2.451	.029	.94	.04256		10.57	15.18	22.0	.272	.0280						
	12-23	1.033	.141	-.746	.131	-.077	.93	.04212		10.63	15.28	19.6	.181	.0330						
Model D; θ_c = 60°; x_{cg}/d = 0.17; d ≈ 5.080 cm																				
1182	6-16	.949	.152	-.651	1.597	0	.89	.1251	.1458	11.25	16.72	16.6	.150	.0241	5.0795	.07649	.06754	.5822	29.222	.1932
	9-19	.912	.152	-.571	1.811	.011	.88	.1231		11.81	16.97	16.3	.157	.0137						
	11-21	.920	.152	-.572	.574	-.031	.87	.1217		11.46	17.03	15.2	.185	.0145						
	15-24	.897	.153	-.625	-1.817	-.114	.85	.1197		11.83	16.87	16.4	.180	.0185						
1183	3-12	1.163	.157	-.960	4.571	.084	1.04	.1472	.1463	7.15	10.47	37.4	.399	.0168	5.0805	.07697	.06813	.5810	29.161	.1927
	7-16	1.232	.159	-.830	7.337	.181	1.02	.1443		7.59	11.02	24.0	.243	.0241						
	9-19	1.191	.157	-.842	4.904	.098	1.00	.1416		8.03	11.61	24.7	.311	.0239						
	11-21	1.166	.155	-.750	3.358	.050	.99	.1396		8.08	11.92	17.3	.364	.0178						
	15-24	1.100	.156	-.786	.216	-.057	.97	.1369		8.52	12.13	18.7	.194	.0297						
1184	4-13	1.363	.146	-.956	-.396	-.093	1.52	.2128	.1452	10.92	13.92	2.0	.204	.0175		.07602	.06709	.5812	29.247	.1937
	7-16	1.363	.146	-.970	-.232	-.088	1.50	.2093		10.84	14.01	2.0	.166	.0150						
	9-18	1.373	.146	-.966	-.665	-.103	1.47	.2058		11.06	14.03	2.0	.148	.0165						
	11-21	1.353	.145	-1.017	-.425	-.096	1.44	.2015		10.84	13.97	2.0	.158	.0137						
	15-24	1.327	.145	-.996	.335	-.068	1.41	.1968		10.66	14.02	2.1	.163	.0178						
1185	7-17	1.300	.142	-.948	.284	-.067	1.33	.1865	.1457	14.80	21.89	20.7	.204	.0236	5.0803	.07642	.06742	.5820	29.258	.1932
	9-19	1.274	.142	-.940	.635	-.054	1.31	.1833		14.89	21.89	20.3	.245	.0236						
	12-22	1.270	.142	-.981	-.018	-.078	1.28	.1792		14.90	21.88	19.6	.262	.0292						
	15-24	1.270	.142	-.996	.175	-.072	1.26	.1764		14.80	21.87	19.0	.271	.0198						
1186	7-17	1.309	.146	-1.076	2.477	.003	1.30	.1819	.1453	11.55	17.25	11.6	.183	.0208		.07697	.06859	.5850	28.960	.1913
	9-19	1.278	.146	-1.096	1.244	-.039	1.28	.1788		12.04	17.30	11.6	.219	.0211						

TABLE 2.- DATA SUMMARY FOR THE TWO BASIC CONFIGURATIONS - Continued.

Run	Sta. Int.	C_D	$-C_{m_\alpha}$, per rad	C_{L_α}, per rad	ξ	$C_{m_q} + C_{m_{\dot\alpha}}$	M_∞	$Re\times10^{-6}$	$\rho_\infty\times10^3$, g/cm³	α_{rms}, deg	α_m, deg	α_m/α_{min}	α,β dev., deg	y,z dev., cm	d, cm	$m\times10^{-3}$, g	$I_y\times10^{-3}$, g-cm²	I_y/I_x	md^2/I_y	$\rho_\infty A/2m\times10^4$, cm⁻¹
1186	12-22	1.292	0.146	-1.059	-0.265	-0.090	1.25	0.1748	0.1453	11.76	17.48	12.2	0.168	0.0211	5.0803	0.07697	0.06859	0.5850	28.960	0.1913
	16-24	1.270	.147	-1.008	-1.373	-.126	1.23	.1717		12.05	17.33	12.9	.289	.0241						
1187	3-14	1.158	.136	-.891	.346	-.059	1.20	.1686	.1454	25.32	38.31	7.6	.476	.0335	5.0851	.07727	.06862	.5814	29.116	.1911
	7-17	1.170	.136	-.890	-.007	-.071	1.18	.1658		25.14	37.95	7.9	.438	.0348						
	9-20	1.162	.137	-.893	-.575	-.090	1.16	.1627		24.55	37.64	8.3	.456	.0366						
	12-22	1.135	.137	-.902	-.451	-.085	1.14	.1600		24.56	37.20	8.2	.245	.0348						
	16-24	1.128	.138	-.921	-1.427	-.119	1.12	.1574		24.89	36.74	8.7	.356	.0175						
1193	6-15	1.391	.156	-1.091	-3.084	-.191	1.62	.2272	.1456	4.03	5.82	8.1	.187	.0150	5.0658	.07514	.06617	.5809	29.141	.1952
	8-18	1.393	.161	-1.122	-1.977	-.154	1.59	.2250		4.07	5.81	9.4	.156	.0190						
	11-21	1.373	.161	-1.130	2.213	-.010	1.55	.2173		3.97	5.76	8.7	.175	.0147						
	14-23	1.360	.160	-1.140	-.916	-.117	1.53	.2136		3.95	5.84	8.9	.151	.0135						
1194	6-16	1.224	.149	-.887	2.282	.006	1.17	.1667	.1468	6.04	8.59	5.3	.145	.0302	5.0800	.07536	.06633	.5807	29.318	.1975
	9-19	1.255	.148	-1.002	4.373	.072	1.15	.1631		6.13	8.89	5.0	.191	.0257						
	11-21	1.270	.147	-1.028	6.870	.156	1.13	.1605		6.52	9.24	4.8	.156	.0277						
	14-24	1.245	.148	-.906	9.230	.241	1.11	.1573		6.95	9.89	4.4	.214	.0215						
1195	7-16	1.447	.158	-.990	10.320	.269	1.10	.1549	.1457	5.31	7.63	5.6	.205	.0208		.07439	.06538	.5818	29.360	.1985
	9-19	1.337	.157	-.988	5.217	.099	1.08	.1521		5.55	8.08	5.4	.135	.0170						
	11-21	1.246	.156	-1.018	4.569	.079	1.06	.1496		5.84	8.33	4.6	.257	.0180						
	15-24	1.236	.157	-1.067	6.799	.153	1.04	.1462		6.19	8.74	4.6	.251	.0210						
1196	7-17	1.256	.150	-.777	3.350	.045	1.06	.1493	.1463	7.91	11.73	33.5	.226	.0206	5.0617	.07677	.06774	.5820	29.038	.1917
	9-19	1.251	.152	-.841	2.535	.015	1.04	.1468		8.10	11.92	29.8	.158	.0185						
	12-22	1.246	.151	-.888	6.027	.134	1.02	.1437		8.52	12.49	78.1	.375	.0229						
	15-24	1.210	.149	-.883	5.427	.115	1.01	.1415		8.65	12.89	322.5	.429	.0221						
Model E; $\theta_c = 60°$; $x_{cg}/d = 0.27$; $d \approx 5.080$ cm																				
1052	3-11	1.332	.155	-.961	15.729	.520	1.16	.3086	.2799	4.24	5.91	4.1	.415	.0178	5.0373	.08889	.08733	.5759	25.829	.3138
	6-14	1.365	.152	-.945	16.020	.531	1.13	.3004		4.75	6.64	3.4	.303	.0208						
	8-17	1.359	.146	-.913	11.920	.374	1.10	.2923		5.54	7.71	3.3	.240	.0173						
	10-19	1.363	.145	-.913	10.332	.312	1.07	.2844		6.20	8.58	3.3	.206	.0183						
	13-21	1.343	.144	-.962	8.987	.259	1.04	.2761		6.92	9.56	3.3	.197	.0129						
	16-23	1.297	.142	-.892	7.102	.190	1.01	.2689		7.53	10.34	3.4	.289	.0117						
	18-24	1.260	.138	-.866	6.017	.151	.99	.2643		8.06	10.93	3.3	.146	.0190						
1062	3-11	1.029	.147	-.930	-.587	-.098	.80	.2119	.2768	9.50	12.61	3.9	.250	.0343	5.0826	.09084	.09023	.5754	26.008	.3091
	6-14	1.022	.149	-.882	.583	-.051	.78	.2077		9.41	12.46	3.9	.217	.0409						
	8-17	1.010	.150	-.886	-.640	-.098	.77	.2036		9.49	12.53	3.8	.248	.0363						
	10-19	1.000	.152	-.946	-.793	-.105	.75	.1995		9.47	12.44	3.5	.248	.0272						
	13-21	1.001	.152	-.853	-1.455	-.127	.73	.1953		9.22	12.16	3.2	.313	.0233						
	16-23	.999	.151	-.663	-3.720	-.207	.72	.1915		8.99	11.76	2.9	.157	.0366						
1063	3-11	1.279	.122	-.964	1.137	-.043	1.39	.3734	.2799	10.16	14.69	10.1	.175	.0363	5.0594	.08970	.08812	.5751	26.058	.3136
	6-14	1.431	.121	-.987	.703	-.066	1.36	.3633		10.42	14.85	9.0	.198	.0340						
	8-17	1.519	.121	-1.068	1.322	-.049	1.32	.3535		10.41	15.00	9.1	.186	.0325						
	10-19	1.380	.122	-1.116	2.058	-.017	1.28	.3433		10.87	15.22	8.7	.214	.0218						
	13-22	1.387	.123	-1.165	2.938	.015	1.23	.3309		10.70	15.83	9.3	.152	.0119						
	17-24	1.374	.123	-1.119	1.967	-.020	1.20	.3204		11.39	16.17	8.0	.191	.0178						
1118	1-9	1.087	.147	-.716	6.462	.180	.94	.2703	.2966	4.71	6.44	20.8	.274	.0183	5.0813	.09120	.09085	.5745	25.919	.3298
	3-11	1.080	.141	-.770	2.909	.041	.92	.2652		4.40	6.51	25.0	.392	.0183						
	6-13	1.088	.148	-.616	3.672	.076	.90	.2602		4.76	6.85	38.1	.662	.0267						
	8-16	1.105	.153	-.702	.448	-.052	.88	.2542		4.59	6.80	21.3	.364	.0150						
	10-18	1.089	.149	-.678	1.030	-.029	.87	.2490		4.84	6.79	14.1	.434	.0155						
	12-21	1.060	.146	-.625	.597	-.042	.84	.2424		4.89	7.08	10.9	.565	.0226						
	15-23	1.077	.153	-.630	.436	-.049	.82	.2371		4.83	6.77	6.4	.399	.0526						
1121	5-12	1.278	.145	-.841	3.017	.035	1.00	.2858	.2968	8.90	12.91	21.9	.328	.0135	5.0399	.08853	.08679	.5798	25.911	.3344
	7-15	1.257	.144	-.829	4.352	.088	.98	.2795		9.17	13.26	22.5	.300	.0223						
	9-18	1.178	.143	-.777	1.586	-.014	.95	.2711		9.29	13.74	32.0	.241	.0236						
	11-20	1.125	.144	-.776	1.696	-.008	.93	.2645		9.43	13.99	43.8	.189	.0203						
	14-22	1.091	.144	-.746	1.806	-.001	.90	.2584		9.61	14.21	355.3	.207	.0178						
1152	5-14	1.374	.126	-1.019	-1.120	-.135	1.37	.3549	.2680	11.91	17.13	27.2	.446	.0188	5.0782	.09082	.09032	.5760	25.931	.2989
	8-17	1.403	.125	-1.061	.513	-.075	1.33	.3441		11.60	17.12	16.2	.283	.0191						
	10-20	1.464	.125	-1.061	1.528	-.039	1.29	.3324		11.80	17.29	14.7	.169	.0180						
	13-23	1.475	.126	-1.081	1.308	-.048	1.24	.3202		12.22	17.40	10.8	.294	.0102						
1153	7-15	1.472	.135	-1.146	18.826	.623	1.52	.4140	.2849	4.93	5.91	1.6	.369	.0124	5.0381	.08852	.08633	.5718	26.026	.3208
	9-18	1.458	.127	-1.216	13.484	.415	1.47	.3998		5.85	6.82	1.5	.175	.0183						
	10-19	1.433	.125	-1.212	12.425	.376	1.44	.3939		6.16	7.32	1.4	.149	.0160						
	13-22	1.520	.137	-1.123	13.429	.414	1.39	.3782		7.46	8.81	1.5	.394	.0294						
	16-24	1.413	.127	-1.161	10.958	.322	1.35	.3677		8.19	9.45	1.4	.465	.0140						

TABLE 2.- DATA SUMMARY FOR THE TWO BASIC CONFIGURATIONS - Continued.

Run	Sta. Int.	C_D	$-C_{m_\alpha}$, per rad	C_{L_α}, per rad	ξ	$C_{m_q} + C_{m_{\dot\alpha}}$	M_∞	$Re\times10^{-6}$	$\rho_\infty\times10^3$, g/cm^3	α_{rms}, deg	α_m, deg	α_m/α_{min}	α,β dev., deg	y,z dev., cm	d, cm	$m\times10^{-3}$, g	$I_y\times10^{-3}$, g-cm^2	I_y/I_x	md^2/I_y	$\rho_\infty A/2m\times10^4$, cm^{-1}
Model F; θ_c = 60°; x_{cg}/d = 0.23; d ≈ 5.080 cm																				
1237	4-15	1.328	0.122	-1.114	0.919	-0.077	1.41	0.4828	0.3540	4.00	4.56	1.3	0.128	0.0170	5.0770	0.1412	0.1829	0.7317	19.904	0.2537
	7-19	1.324	.118	-1.135	1.852	-.031	1.37	.4692		4.14	4.65	1.3	.156	.0193						
	10-22	1.306	.113	-1.228	1.581	-.048	1.32	.4536		4.18	4.75	1.3	.180	.0264						
	13-24	1.301	.114	-1.162	-1.830	-.216	1.29	.4434		4.12	4.73	1.4	.215	.0307						
1238	2-14	1.301	.118	-.991	-5.416	-.389	1.27	.4398	.3567	2.00	2.71	2.4	.180	.0297	5.0782	.1423	.1851	.7307	19.829	.2539
	7-18	1.302	.124	-.877	-8.870	-.557	1.23	.4254		1.88	2.42	2.0	.164	.0274						
	9-21	1.283	.129	-.386	-6.432	-.409	1.19	.4137		1.73	2.24	2.0	.136	.0366						
	13-24	1.270	.122	-1.342	-5.565	-.412	1.16	.4004		1.59	2.08	2.1	.151	.0310						
1239	4-15	1.245	.122	-.971	-3.903	-.310	1.10	.3719	.3494	7.54	9.91	2.4	.250	.0213	5.0777	.1456	.1899	.7317	19.769	.2430
	7-19	1.245	.122	-.967	-4.051	-.317	1.07	.3624		7.18	9.45	2.4	.251	.0381						
	10-22	1.248	.126	-.998	-4.595	-.346	1.04	.3514		6.68	8.93	2.5	.271	.0340						
	13-24	1.240	.126	-1.065	-3.007	-.269	1.02	.3442		6.81	8.80	2.6	.330	.0295						
1240	7-18	1.281	.117	-.722	1.804	-.010	1.06	.3554	.3475	1.32	1.93	38.6	.210	.0155	5.0782	.1414	.1836	.7308	19.864	.2488
	9-21	1.256	.115	-1.132	-3.747	-.309	1.03	.3461		1.30	1.81	45.3	.220	.0368						
	13-24	1.211	.121	-.680	-.942	-.143	1.00	.3354		1.23	1.80	22.5	.262	.0368						
1241	3-14	1.268	.123	-1.041	-2.382	-.237	1.18	.4002	.3516	7.09	10.33	9.5	.225	.0206	5.0739	.1413	.1837	.7322	19.800	.2516
	7-18	1.270	.122	-1.055	-1.420	-.189	1.14	.3889		6.97	10.10	11.0	.140	.0157						
	9-21	1.255	.123	-1.077	-1.498	-.193	1.11	.3785		6.68	9.90	10.8	.180	.0323						
	13-24	1.252	.124	-1.095	-2.836	-.262	1.08	.3666		6.63	9.59	12.5	.147	.0142						
1242	3-15	1.258	.117	-1.054	-7.233	-.481	1.06	.3582	.3507	2.99	4.48	19.5	.115	.0122	5.0767	.1429	.1857	.7292	19.841	.2483
	7-19	1.253	.118	-1.013	-8.523	-.544	1.03	.3476		2.82	4.09	24.1	.167	.0366						
	10-22	1.186	.114	-1.013	-4.242	-.325	1.00	.3372		2.57	3.76	41.8	.252	.0287						
	13-24	1.129	.114	-.994	-4.772	-.348	.98	.3305		2.48	3.61	120.4	.227	.0147						
(b) Aerodynamic Facility																				
Model A; θ_c = 55°; x_{cg}/d = 0.17; d ≈ 2.032 cm																				
270	1-9	1.322	0.158	-0.991	17.539	0.651	1.14	0.1511	0.3451	6.62	8.29	1.7	0.431	0.0114	2.0340	0.01291	0.002285	0.5492	23.373	0.4343
	3-11	1.307	.149	-.980	18.358	.688	1.12	.1485		7.55	9.41	1.7	.319	.0107						
	6-14	1.302	.147	-1.127	11.762	.399	1.09	.1447		8.48	10.48	1.6	.323	.0102						
	7-16	1.304	.155	-1.133	7.870	.232	1.08	.1429		9.17	11.04	1.6	.296	.0086						
271	3-11	1.335	.157	-.992	11.544	.395	1.17	.1559	.3450	5.39	7.97	8.5	.301	.0081	2.0345	.01285	.002281	.5497	23.326	.4363
	5-14	1.327	.158	-1.122	10.679	.353	1.15	.1525		6.24	8.79	5.7	.541	.0173						
	8-16	1.316	.159	-1.111	10.067	.328	1.12	.1492		6.65	9.35	4.6	.612	.0137						
272	1-9	1.311	.171	-1.298	14.554	.511	1.14	.1525	.3457	4.44	5.70	2.4	.286	.0084	2.0343	.01287	.002277	.5486	23.395	.4365
	3-11	1.310	.167	-1.144	20.147	.756	1.13	.1498		4.99	6.62	2.4	.287	.0081						
	5-13	1.304	.157	-1.075	18.939	.708	1.11	.1473		5.52	7.36	2.3	.545	.0056						
	7-15	1.303	.146	-.904	22.247	.857	1.09	.1447		6.31	8.70	2.3	.289	.0127						
	9-16	1.300	.147	-.990	15.337	.558	1.07	.1429		6.86	8.94	2.3	.605	.0124						
273	1-9	1.068	.162	-.950	-.281	-.098	.93	.1243		3.09	4.15	2.6	.314	.0079	2.0345	.01286	.002275	.5475	23.394	.4371
	4-12	1.028	.161	-.565	-6.492	-.346	.91	.1218		3.10	4.28	3.0	.326	.0119						
	6-14	1.023	.168	-.590	-.978	-.111	.90	.1201		3.00	4.21	3.8	.195	.0069						
	9-16	1.028	.162	-.694	1.947	.010	.89	.1181		2.94	4.08	4.0	.209	.0066						
274	1-8	1.303	.166	-1.090	21.279	.810	1.09	.1448	.3458	5.19	7.18	2.9	.221	.0112	2.0348	.01289	.002289	.5491	23.314	.4362
	3-11	1.297	.164	-1.135	17.145	.631	1.06	.1417		6.07	8.36	2.9	.188	.0104						
	5-13	1.283	.161	-.997	17.725	.663	1.05	.1393		6.76	9.40	2.6	.285	.0155						
	7-15	1.263	.161	-.911	13.471	.485	1.03	.1370		7.55	10.11	2.5	.406	.0086						
	9-16	1.231	.163	-.950	9.852	.329	1.02	.1353		8.17	10.61	2.4	.317	.0086						
275	1-9	1.305	.169	-.848	28.941	1.150	1.10	.1475	.3463	3.89	5.47	3.0	.384	.0076	2.0345		.002291	.5487	23.294	.4368
	3-12	1.299	.167	-.883	16.080	.597	1.08	.1443		4.55	6.21	2.9	.318	.0107						
	6-14	1.290	.169	-1.066	11.253	.382	1.06	.1412		5.05	7.00	2.9	.240	.0203						
	8-16	1.276	.165	-1.062	10.487	.350	1.04	.1388		5.49	7.57	2.7	.177	.0185						
279	1-10	1.266	.144	-1.032	1.331	-.041	1.12	.1492	.3450	17.00	24.63	24.9	.412	.0124	2.0366	.01312	.002367	.5484	22.996	.4283
	4-12	1.255	.144	-.968	1.188	-.045	1.10	.1462		17.14	24.68	22.3	.450	.0086						
	7-15	1.271	.147	-.988	1.246	-.044	1.07	.1426		17.11	25.10	19.6	.562	.0089						
	9-16	1.272	.149	-.985	1.539	-.031	1.06	.1408		17.94	25.32	18.5	.285	.0104						
280	1-9	1.227	.182	-.855	12.987	.473	.98	.1300	.3444	3.97	5.49	39.3	.415	.0104	2.0330	.01304	.002338	.5472	23.047	.4288
	2-10	1.232	.177	-1.038	8.685	.278	.97	.1290		3.88	5.77	64.1	.254	.0130						

TABLE 2.- DATA SUMMARY FOR THE TWO BASIC CONFIGURATIONS - Continued.

Run	Sta. Int.	C_D	$-C_{m_\alpha}$, per rad	C_{L_α}, per rad	ξ	$C_{m_q} + C_{m_{\dot\alpha}}$	M_∞	$Re\times10^{-6}$	$\rho_\infty\times10^3$, g/cm^3	α_{rms}, deg	α_m, deg	α_m/α_{min}	α,β dev., deg	y,z dev., cm	d, cm	$m\times10^{-3}$, g	$I_y\times10^{-3}$, g-cm^2	I_y/I_x	md^2/I_y	$\rho_\infty A/2m\times10^2$, cm^{-1}
280	4-12	1.194	0.177	-1.121	7.714	0.234	0.96	0.1270	0.3444	4.17	6.06	19.6	0.208	0.0142	2.0330	0.01304	0.002338	0.5472	23.047	0.4288
	7-14	1.097	.169	-.988	4.189	.091	.94	.1246		4.36	6.34	20.5	.386	.0145						
	9-16	1.053	.163	-.958	.308	-.074	.93	.1229		4.69	6.60	17.4	.234	.0132						
281	1-9	1.325	.161	-1.015	21.843	.823	1.10	.1339	.3163	5.34	6.37	1.6	.232	.0099	2.0345	.01337	.002334	.5489	23.709	.3846
	2-10	1.318	.156	-1.247	20.194	.744	1.09	.1328		5.67	6.86	1.5	.166	.0208						
	4-12	1.308	.158	-1.209	16.641	.596	1.07	.1308		6.47	7.50	1.5	.220	.0114						
	6-14	1.317	.155	-1.356	16.228	.572	1.06	.1288		7.18	8.17	1.4	.271	.0124						
	8-16	1.310	.151	-1.265	14.583	.506	1.04	.1268		7.80	8.80	1.3	.265	.0135						
282	1-9	1.328	.154	-.899	33.465	1.336	1.17	.1425	.3156	4.99	6.89	2.7	.510	.0096	2.0343	.01288	.002280	.5481	23.382	.3981
	3-12	1.315	.149	-.777	25.168	.987	1.15	.1397		5.98	8.11	2.2	.541	.0119						
	6-14	1.310	.147	-.968	12.758	.448	1.13	.1369		7.34	9.43	2.0	.240	.0152						
	6-16	1.309	.147	-.961	13.479	.479	1.12	.1358		7.77	9.78	1.9	.316	.0142						
	8-16	1.311	.147	-.935	11.143	.381	1.11	.1348		7.92	10.09	1.9	.162	.0071						
Model B; θ_c = 55°; x_{cg}/d = 0.20; d ≈ 2.032 cm																				
120	1-12	0.987	0.173	-0.818	0.381	-0.073	0.84	0.0357	0.1105	12.58	18.31	12.8	0.193	0.0200	2.0333	0.007084	0.001491	0.6583	19.638	0.2532
	5-16	.977	.172	-.828	1.465	-.017	.83	.0351		12.39	18.41	15.9	.239	.0140						
122	3-13	.901	.158	-.601	2.393	.042	.71	.0295	.1094	15.33	22.45	24.2	.223	.0190	2.0279	.007018	.001353	.6590	21.325	.2518
	6-16	.897	.158	-.558	2.776	.062	.70	.0292		15.53	22.75	23.0	.206	.0183						
128	1-12	.928	.164	-.643	.191	-.066	.67	.0280	.1097	13.52	16.65	1.7	.257	.0163	2.0297	.007276	.001438	.6435	20.841	.2439
	5-16	.921	.164	-.618	.662	-.042	.66	.0276		13.33	16.53	1.7	.234	.0155						
Model C; θ_c = 60°; x_{cg}/d = 0.23; d ≈ 2.032 cm																				
231	1-9	1.243	0.119	-1.085	1.454	-0.041	1.21	0.2431	0.5208	16.70	24.50	350.0	0.345	0.0094	2.0351	0.01440	0.002799	0.5554	21.299	0.5884
	4-12	1.230	.120	-1.048	.702	-.074	1.17	.2352		16.86	24.87	108.1	.372	.0107						
	6-14	1.212	.120	-1.056	1.139	-.053	1.15	.2301		16.62	24.99	75.8	.344	.0114						
	8-16	1.206	.121	-1.039	2.024	-.010	1.12	.2251		17.58	25.28	41.5	.196	.0135						
232	1-9	1.220	.123	-1.008	2.062	-.008	1.17	.2332	.5183	18.79	27.37	34.7	.667	.0223	2.0328	.01443	.002802	.5555	21.277	.5828
	4-12	1.208	.125	-.999	1.830	-.018	1.13	.2258		18.99	27.98	26.4	.382	.0127						
	6-14	1.196	.124	-.985	2.316	.006	1.11	.2210		18.76	28.26	21.1	.337	.0145						
	8-16	1.200	.124	-.990	1.208	-.046	1.09	.2164		19.33	28.21	20.2	.414	.0135						
233	1-9	1.269	.126	-1.136	1.584	-.039	1.16	.2336	.5214	8.39	12.48	124.8	.547	.0058	2.0343	.01456	.002841	.5546	21.206	.5820
	4-12	1.258	.129	-1.203	4.847	.113	1.13	.2259		9.07	12.94	30.8	.237	.0051						
	6-14	1.250	.129	-1.137	6.773	.207	1.10	.2209		9.00	13.53	18.0	.387	.0124						
	8-16	1.238	.127	-1.049	6.262	.188	1.08	.2161		9.77	14.28	16.2	.298	.0058						
234	1-9	.963	.129	-.713	2.131	.021	.92	.1828	.5172	14.97	22.23	21.2	.276	.0101	2.0340	.01453	.002828	.5539	21.252	.5785
	3-11	.948	.129	-.685	2.449	.038	.91	.1797		15.22	22.69	24.4	.203	.0132						
	6-14	.936	.129	-.697	1.463	-.008	.88	.1753		15.82	23.24	27.0	.229	.0119						
	8-16	.930	.130	-.656	.659	-.044	.87	.1724		15.29	23.20	26.1	.356	.0180						
258	1-8	1.215	.118	-1.059	.581	-.079	1.16	.2739	.6070	12.17	17.73	59.1	.335	.0053	2.0325	.01428	.002752	.5501	21.437	.6895
	1-11	1.209	.119	-1.027	2.921	.032	1.14	.2687		12.50	18.29	166.4	.477	.0150						
	3-11	1.205	.121	-1.034	3.343	.052	1.13	.2654		12.52	18.46	92.3	.404	.0124						
	5-13	1.193	.120	-.974	4.059	.088	1.10	.2588		12.79	19.02	52.6	.275	.0160						
	7-15	1.185	.122	-.937	3.320	.056	1.07	.2523		13.32	19.55	34.9	.469	.0097						
	10-16	1.165	.124	-1.061	1.727	-.023	1.04	.2462		14.36	19.97	31.7	.213	.0101						
259	1-9	.980	.128	-.592	-4.151	-.266	.90	.2086	.5995	5.58	7.75	12.7	.133	.0094	2.0335	.01424	.002742	.5512	21.480	.6836
	2-10	.972	.131	-.675	-.666	-.108	.89	.2065		5.53	7.92	12.0	.231	.0122						
	4-12	.952	.131	-1.025	.715	-.059	.87	.2024		5.54	7.87	12.5	.199	.0314						
	6-14	.932	.130	-1.070	1.141	-.040	.85	.1984		5.44	7.72	13.6	.217	.0185						
	9-16	.919	.130	-.924	-5.234	-.329	.83	.1937		5.21	7.61	12.7	.237	.0140						
260	1-8	1.255	.124	-1.046	.261	-.096	1.16	.2615	.5867	12.76	18.47	370.0	.508	.0117	2.0315	.01434	.002785	.5541	21.253	.6629
	3-11	1.253	.125	-1.067	1.893	-.020	1.12	.2534		12.69	18.74	312.8	.469	.0114						
	5-13	1.248	.127	-1.079	2.638	.015	1.09	.2471		12.83	18.94	379.0	.491	.0127						
	7-15	1.244	.129	-1.056	3.371	.050	1.07	.2409		13.20	19.43	81.0	.451	.0180						
	10-16	1.229	.130	-1.003	3.483	.059	1.04	.2350		14.20	19.88	33.7	.271	.0096						
261	1-8	1.223	.139	-.883	4.994	.135	1.02	.2285	.5848	9.14	13.20	15.2	.440	.0211	2.0330	.01447	.002804	.5524	21.323	.6561
	3-11	1.166	.141	-.907	3.561	.070	.99	.2218		9.95	13.87	22.0	.298	.0192						
	5-12	1.134	.139	-.935	.734	-.063	.97	.2181		9.52	14.00	24.6	.226	.0122						
	7-14	1.082	.140	-.852	-.134	-.097	.95	.2132		9.57	14.20	25.8	.151	.0081						
	9-16	1.033	.138	-.755	-1.384	-.149	.93	.2087		9.79	14.30	22.7	.259	.0063						
276	1-8	1.233	.161	-1.007	11.756	.446	1.05	.2360	.5844	5.84	6.39	1.2	.370	.0122		.01443	.002795	.5520	21.335	.6574
	3-11	1.205	.161	-.928	11.040	.418	1.02	.2289		6.57	7.12	1.2	.384	.0117						
	4-13	1.181	.138	-1.034	7.809	.262	1.00	.2248		7.07	7.47	1.1	.282	.0157						

TABLE 2.- DATA SUMMARY FOR THE TWO BASIC CONFIGURATIONS - Concluded.

Run	Sta. Int.	C_D	$-C_{m_\alpha}$, per rad	C_{L_α}, per rad	ξ	$C_{m_q} + C_{m_{\dot\alpha}}$	M_∞	$Re\times10^{-6}$	$\rho_\infty\times10^3$, g/cm^3	α_{rms}, deg	α_m, deg	α_m/α_{min}	α,β dev., deg	y,z dev., cm	d, cm	$m\times10^{-3}$, g	$I_y\times10^{-3}$, g-cm^2	I_y/I_x	md^2/I_y	$\rho_\infty A/2m\times10^4$, cm^{-1}
276	5-13	1.172	0.145	-1.004	8.133	0.279	0.99	0.2235	0.5844	7.20	7.56	1.1	0.201	0.0152	2.0330	0.01443	0.002795	0.5520	21.335	0.6574
↓	7-15	1.133	.138	-1.039	6.536	.205	.97	.2184	↓	7.58	7.98	1.1	.339	.0094	↓	↓	↓	↓	↓	↓
↓	8-16	1.110	.148	-.980	4.357	.106	.96	.2159	↓	7.76	8.11	1.1	.219	.0102	↓	↓	↓	↓	↓	↓
277	1-9	1.239	.151	-1.143	10.541	.381	1.02	.2304	.5851	4.97	5.95	1.5	.295	.0091	2.0353	↓	.002791	.5517	21.421	.6595
↓	3-12	1.195	.151	-1.134	12.098	.456	.99	.2235	↓	5.95	7.16	1.6	.442	.0117	↓	↓	↓	↓	↓	↓
↓	5-14	1.154	.148	-.990	11.986	.460	.97	.2183	↓	6.64	8.04	1.7	.520	.0145	↓	↓	↓	↓	↓	↓
↓	6-15	1.146	.138	-.948	5.657	.166	.96	.2158	↓	6.80	8.45	1.7	.548	.0124	↓	↓	↓	↓	↓	↓
225	2-11	1.392	.123	-1.139	-1.469	-.190	1.63	.1221	.1959	12.81	19.33	69.1	.236	.0135	2.0302	.006720	.001314	.5498	21.082	.4719
↓	5-13	1.384	.123	-1.158	.032	-.119	1.59	.1191	↓	13.53	19.15	46.7	.300	.0102	↓	↓	↓	↓	↓	↓
↓	7-16	1.383	.124	-1.134	-.771	-.156	1.55	.1162	↓	12.53	18.76	36.1	.395	.0094	↓	↓	↓	↓	↓	↓
226	1-10	1.288	.134	-1.078	15.259	.606	1.14	.0862	.1965	5.81	8.31	9.4	.343	.0058	2.0330	.006695	.001301	.5525	21.271	.4764
↓	6-14	1.285	.134	-1.086	10.257	.371	1.12	.0846	↓	6.17	8.63	7.3	.275	.0099	↓	↓	↓	↓	↓	↓
↓	9-16	1.286	.132	-1.157	2.475	.002	1.09	.0827	↓	6.68	9.27	6.5	.411	.0107	↓	↓	↓	↓	↓	↓
↓	4-12	1.304	.138	-1.187	8.069	.262	1.17	.0883	↓	5.06	7.45	12.6	.367	.0157	↓	↓	↓	↓	↓	↓
227	1-10	1.232	.141	-.976	3.306	.052	.98	.0746	.1973	15.24	22.26	23.2	.264	.0284	2.0351	.006748	.001319	.5514	21.186	.4754
↓	4-13	1.151	.141	-.837	3.151	.055	.96	.0727	↓	15.63	22.86	19.4	.281	.0305	↓	↓	↓	↓	↓	↓
↓	7-15	1.042	.138	-.713	2.554	.038	.94	.0713	↓	15.92	23.08	15.6	.410	.0170	↓	↓	↓	↓	↓	↓
235	2-11	1.159	.130	-.915	3.071	.047	.97	.0733	.1968	17.84	26.45	661.5	.220	.0410	2.0328	.006777	.001317	.5513	21.264	.4712
↓	5-13	1.058	.129	-.770	.551	-.060	.95	.0718	↓	18.23	26.83	111.8	.402	.0366	↓	↓	↓	↓	↓	↓
↓	7-16	.975	.127	-.702	-.279	-.092	.93	.0705	↓	18.00	27.08	69.4	.348	.0127	↓	↓	↓	↓	↓	↓
278	1-9	1.256	.173	-.879	9.118	.327	1.07	.0820	.1982	4.01	5.61	9.2	.278	.0071	2.0335	.006709	.001300	.5484	21.387	.4798
↓	3-11	1.246	.169	-.865	9.650	.353	1.05	.0805	↓	4.31	6.16	8.2	.224	.0079	↓	↓	↓	↓	↓	↓
↓	5-13	1.228	.168	-.952	10.364	.384	1.04	.0790	↓	4.53	6.62	7.9	.339	.0099	↓	↓	↓	↓	↓	↓
↓	7-15	1.192	.160	-.940	9.858	.362	1.02	.0777	↓	4.80	7.10	12.0	.509	.0058	↓	↓	↓	↓	↓	↓
Model C; θ_c = 60°; x_{cg}/d = 0.23; d ≈ 5.080 cm																				
447	1-12	1.209	0.129	-0.918	0.336	-0.084	1.09	0.2613	0.2488	17.69	25.85	16.3	0.466	0.0353	5.0820	0.03622	0.04380	0.5453	21.358	0.6966
↓	4-15	1.146	.129	-.960	.139	-.092	1.05	.2518	↓	17.83	26.11	18.5	.313	.0699	↓	↓	↓	↓	↓	↓
448	1-13	1.054	.129	-.781	-.688	-.118	.99	.2362	↓	24.75	35.02	9.5	.711	.0363	↓	.03638	.04397	.5437	21.371	.6935
449	1-11	1.177	.126	-.908	.248	-.086	1.10	.2916	.2761	23.27	33.42	14.5	.542	.0279	↓	.03641	.04400	.5440	↓	.7691
↓	4-14	1.111	.127	-.875	-.171	-.101	1.06	.2801	↓	23.33	33.55	15.2	.274	.0360	↓	↓	↓	↓	↓	↓
450	2-12	1.205	.129	-.961	1.749	-.020	1.10	.2867	.2730	16.71	24.15	53.7	.612	.0541	↓	.03644	.04421	.5452	21.290	.7598
↓	5-15	1.127	.129	-.875	2.676	.032	1.05	.2753	↓	17.49	25.23	37.1	.411	.0581	↓	↓	↓	↓	↓	↓
483	1-12	1.213	.140	-1.090	4.254	.091	1.08	.2560	.2479	8.03	11.91	15.7	.526	.0338	5.0805	.03593	.04316	.5451	21.484	.6994
↓	4-15	1.135	.141	-.977	3.534	.066	1.04	.2466	↓	8.44	12.34	12.0	.538	.0318	↓	↓	↓	↓	↓	↓
488	1-12	1.317	.136	-1.076	3.269	.041	1.32	.3145	.2488	8.91	11.88	2.8	.345	.0279	5.0795	.03576	.04314	.5448	21.387	.7050
↓	4-15	1.300	.134	-1.003	3.153	.040	1.26	.3014	↓	9.22	12.52	2.7	.281	.0218	↓	↓	↓	↓	↓	↓
489	1-12	.766	.130	-.503	1.319	.002	.65	.1554	.2481	21.83	31.87	91.0	.472	.0325	5.0818	.03558	.04285	.5443	21.442	.7072
↓	4-15	.756	.129	-.492	.413	-.039	.64	.1516	↓	21.73	32.29	52.9	.335	.0378	↓	↓	↓	↓	↓	↓
492	1-11	1.277	.132	-.965	.447	-.084	1.21	.2885	.2480	12.34	17.03	4.0	.314	.0302	5.0836	.03553	↓	↓	21.428	.7084
↓	4-15	1.256	.133	-.931	1.512	-.015	1.16	.2750	↓	12.21	17.51	4.0	.587	.0274	↓	↓	↓	↓	↓	↓

TABLE 3.- TEST CONDITIONS USED IN EVALUATING THE EFFECT OF FACILITY, REYNOLDS NUMBER, AND BLOCKAGE ON THE AERODYNAMIC CHARACTERISTICS OF MODEL C

Symbols used in figures 8-11	Facility	Range diam or equivalent circular diam, M	Range cross-sectional shape	Location of instrumentation and optics	Model maximum diam, cm	Blockage factor, percent 100×Am/Ar	Reynolds number (based on d) $\times 10^{-6}$	ρ_∞, g/cm^3
○	Aero HFF	1.1763	Octagonal	External to test section	2.03	0.0298	0.23	0.56
○́	"	"	"	"	"	"	.08	.20
●	"	"	"	"	5.08	.1865	.27	.25
□	PBR	3.0480	Circular	Internal to range	"	.0278	.27	.28
⧄	"	"	"	"	2.03	.0044	.04	.12

TABLE 4.- WAKE DIMENSIONS

Model configuration	C	C	F	F
Mach No.	0.99	1.08	0.99	1.08
dw/d, at d = 1 (from model nose)	1.45	1.44	1.41	1.33
dw/d, at d = 2 (from model nose)	1.58	1.52	1.35	1.23
x_w/d, at recompression shock (from model nose)	3.65	4.43	3.42	3.51

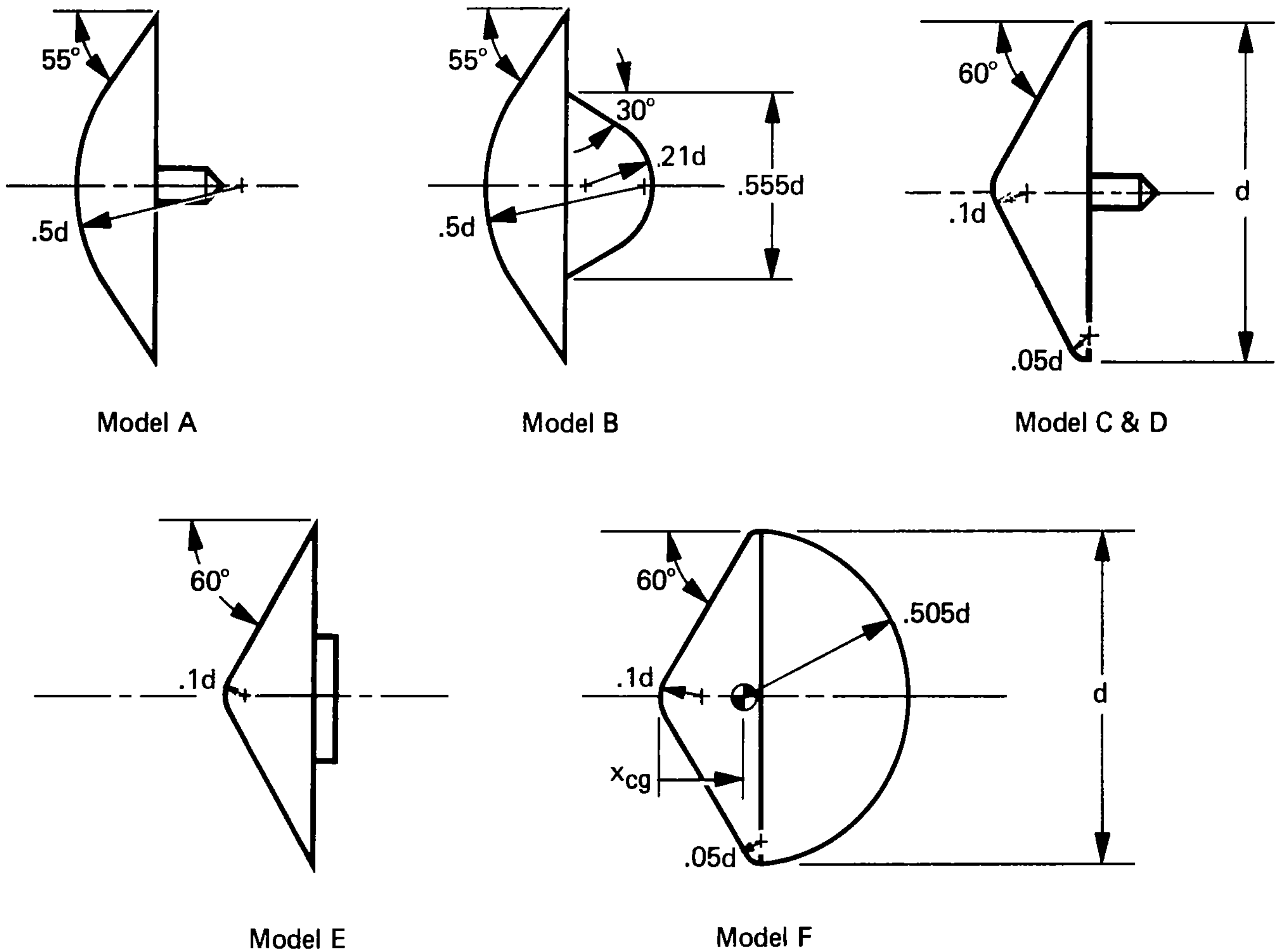

Figure 1.- Model configurations.

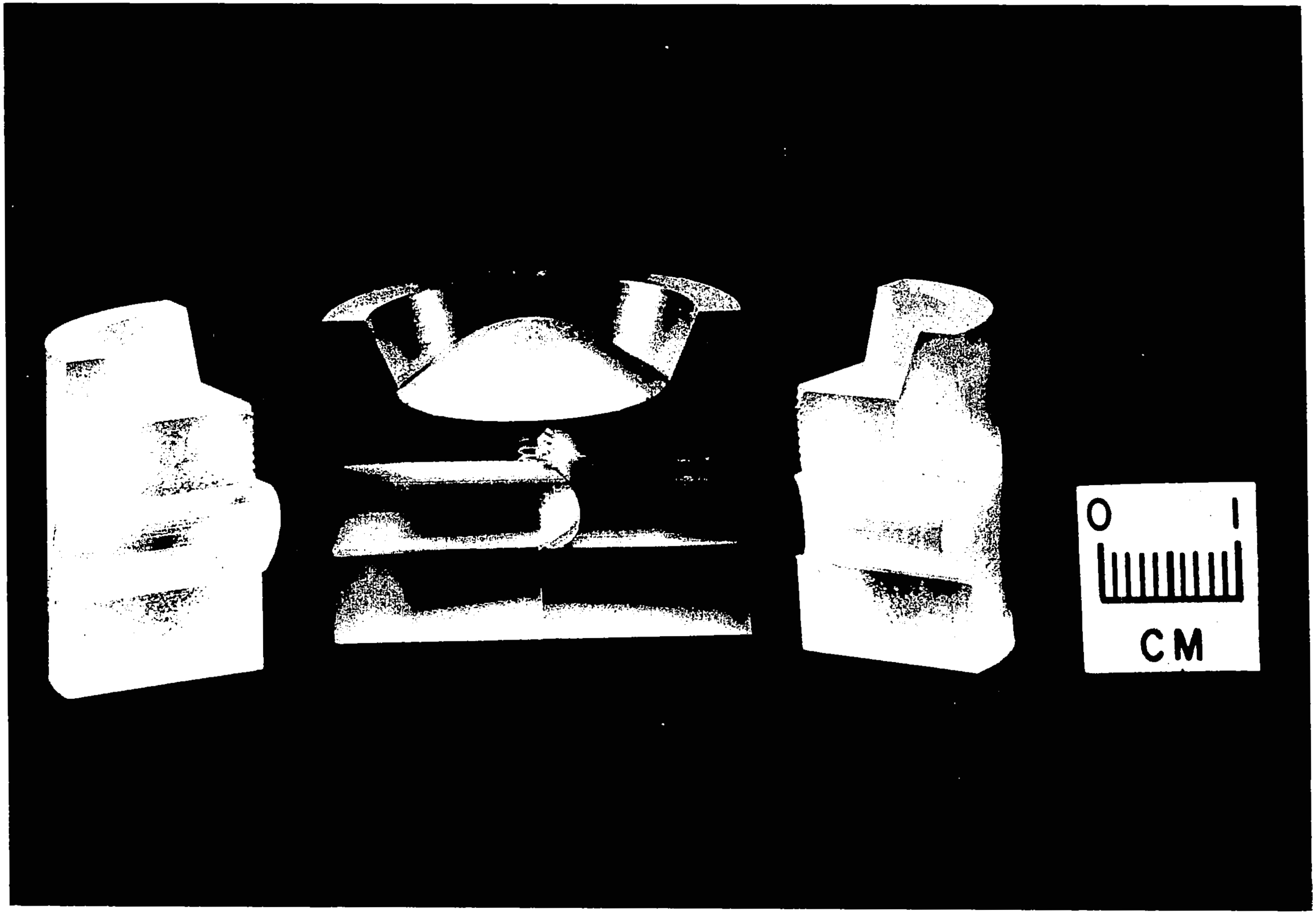

A-36131

(a) Model A with four-piece sabot.

Figure 2.- Models and typical sabots.

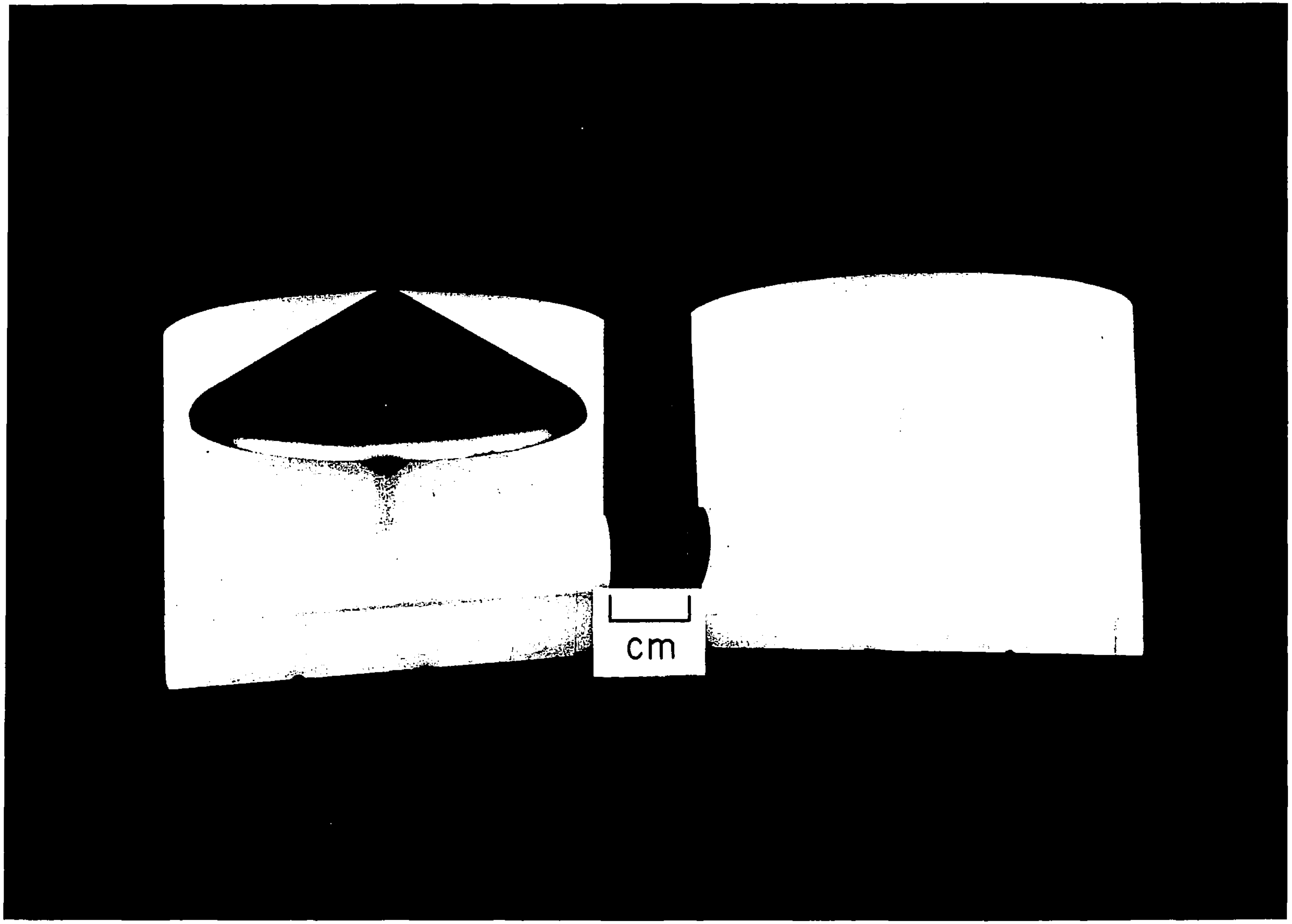

A-38031

(b) Model C with two-piece sabot.

Figure 2.- Continued.

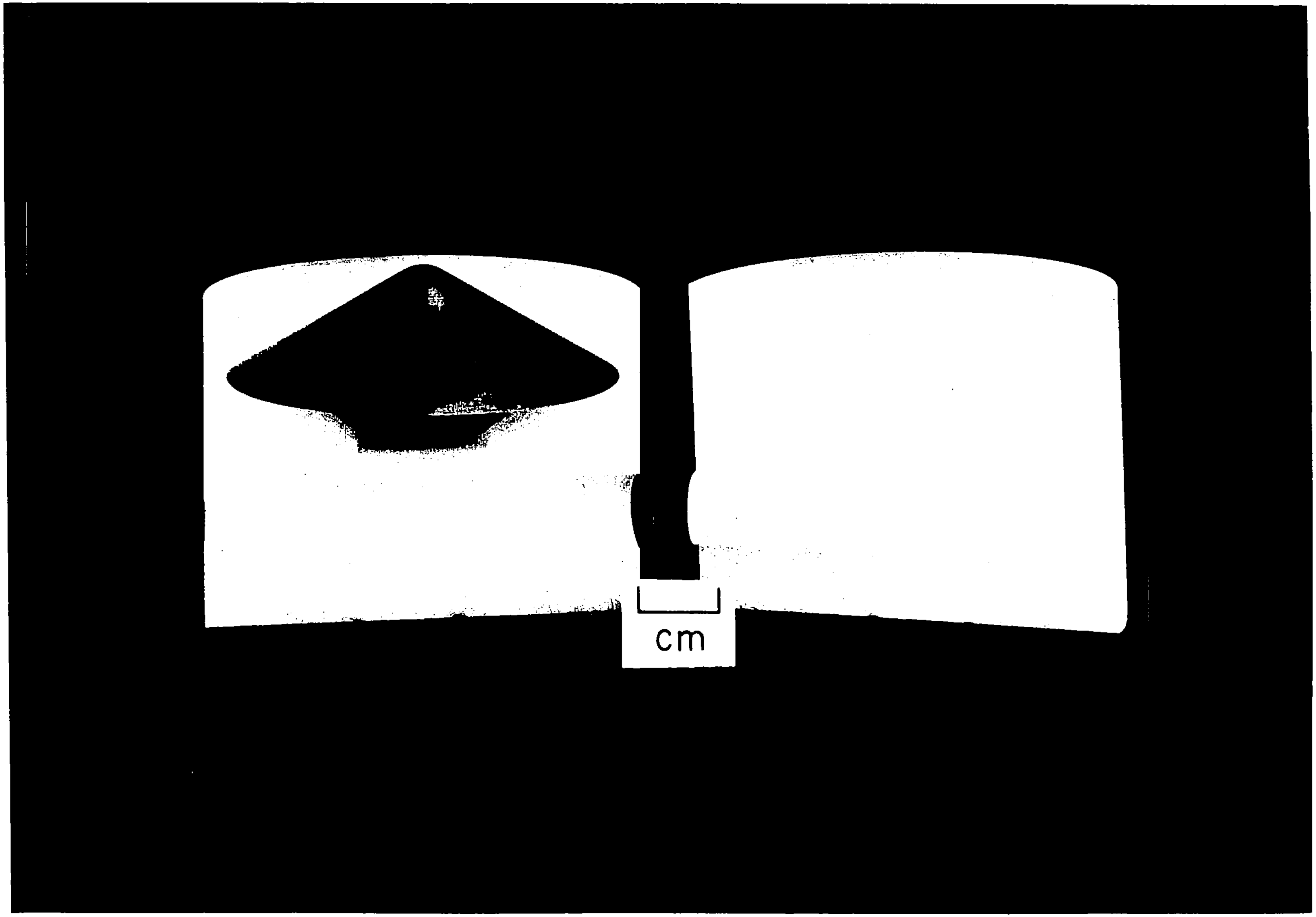

A-38032

(c) Model E with two-piece sabot.

Figure 2.- Continued.

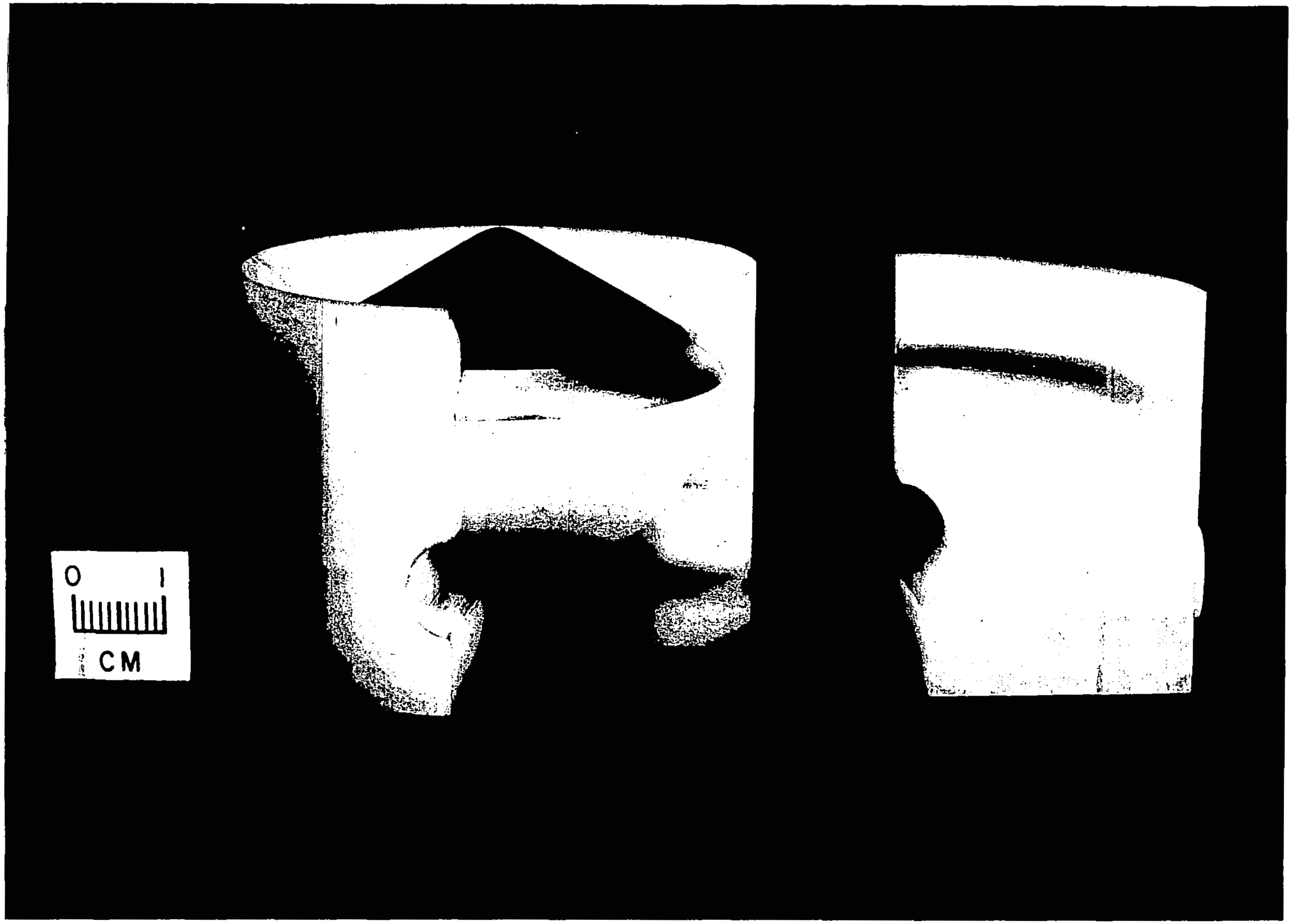

A-40080

(d) Model F with four-piece sabot.

Figure 2.- Continued.

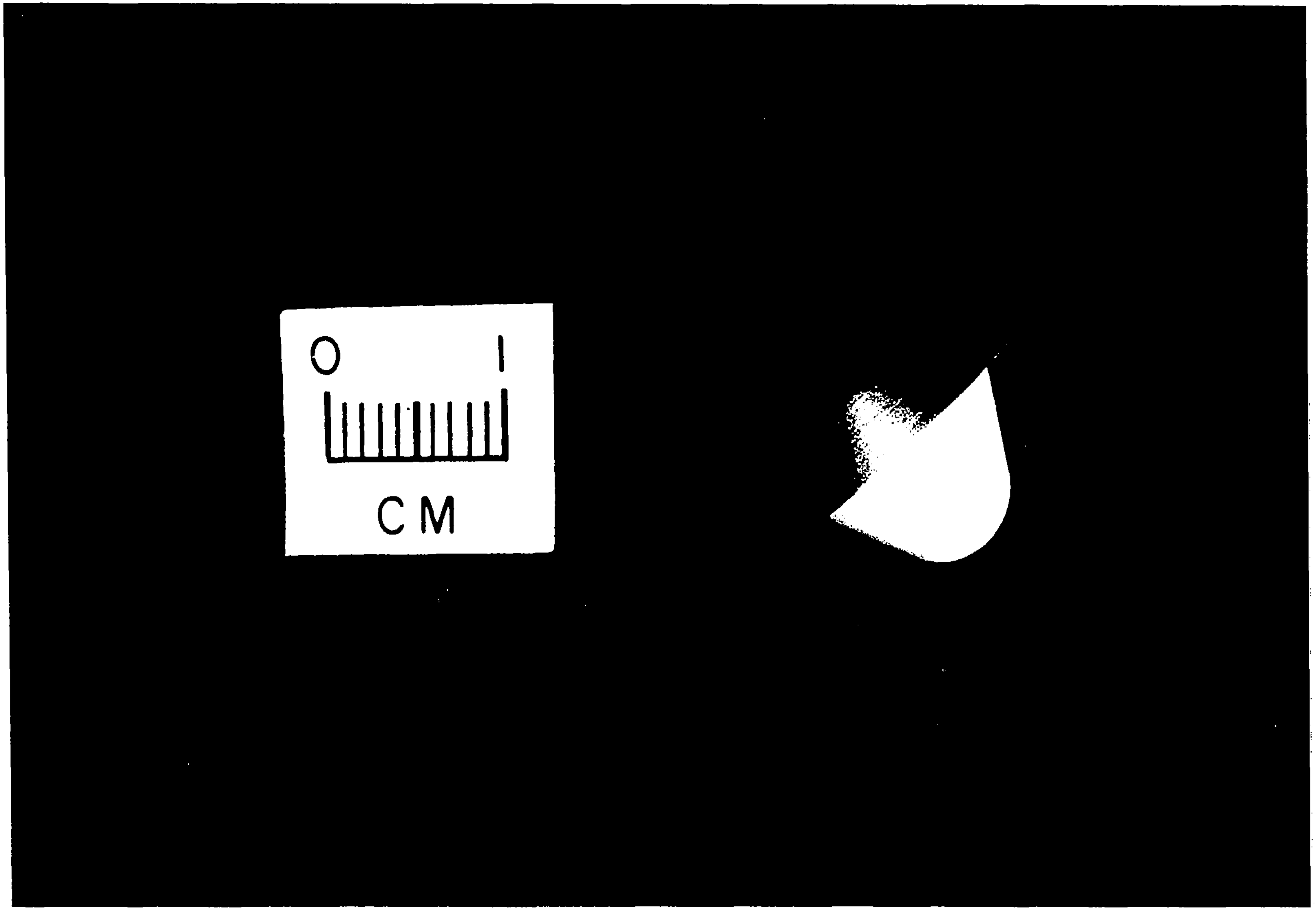

A-40078

(e) Model B.

Figure 2.- Concluded.

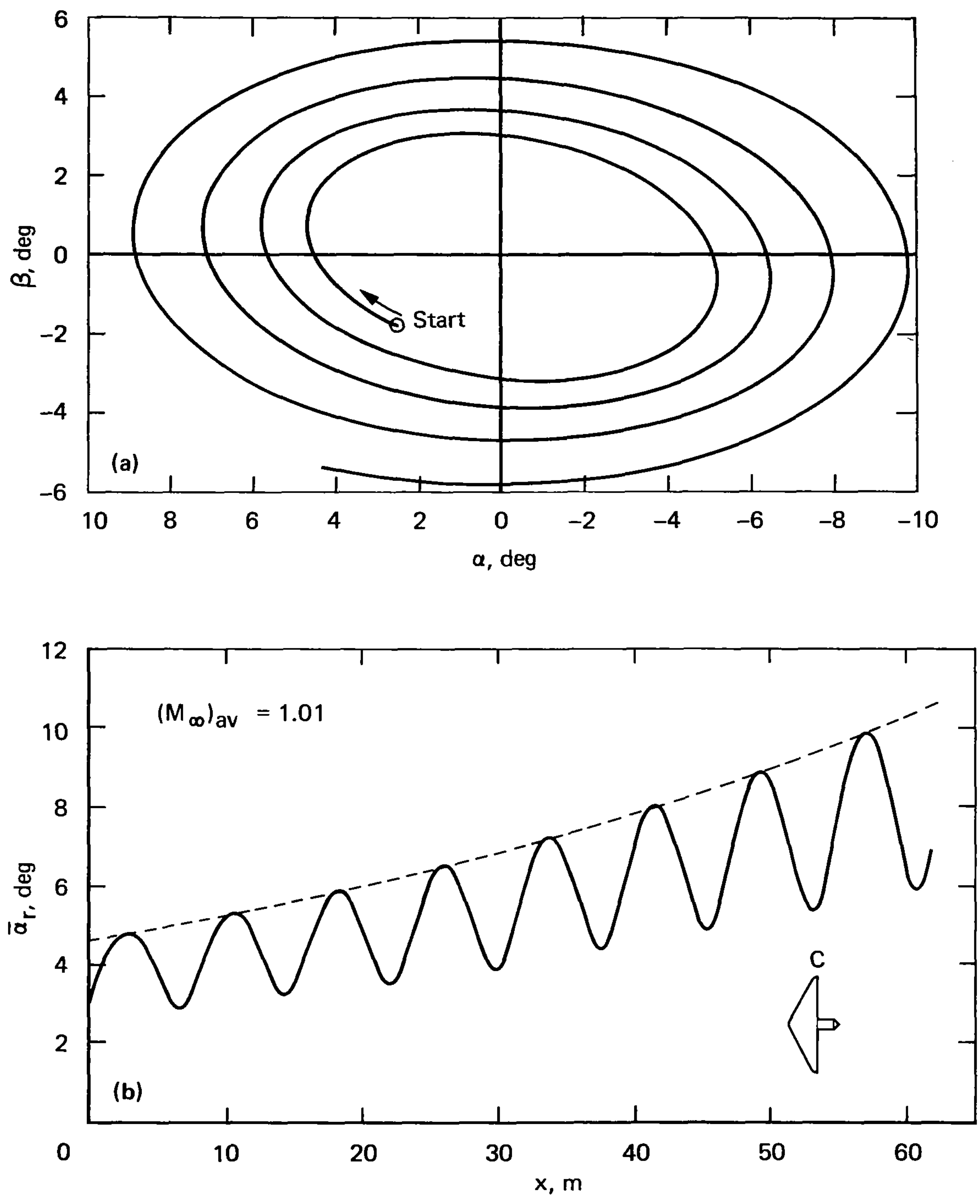

(a) β vs α
(b) $\overline{\alpha}_r$ vs x

Figure 3.- Typical model motion obtained in Pressurized Ballistic Range.

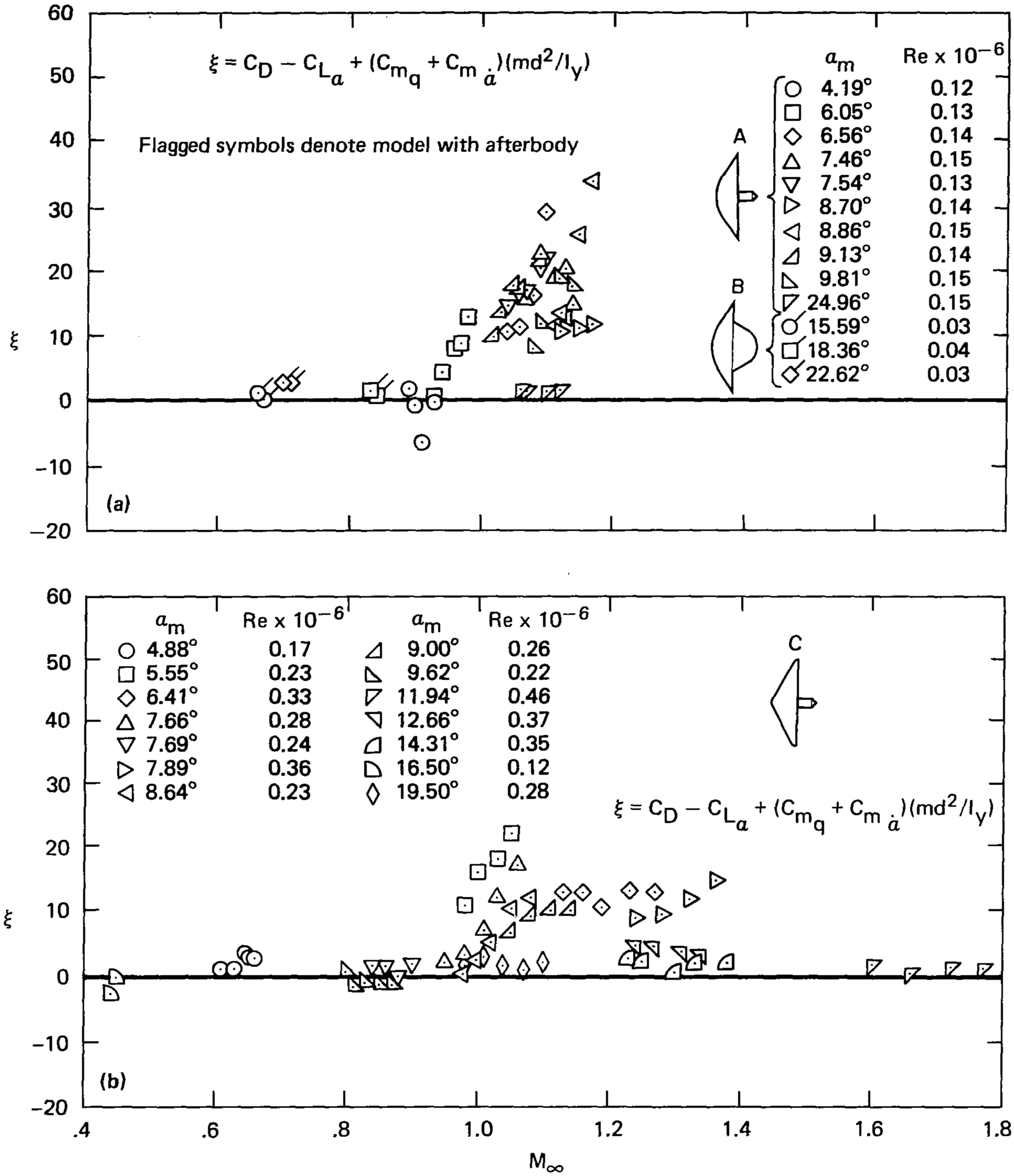

(a) Models A and B.
(b) Model C.

Figure 4.- Variation of the damping parameter (ξ) with M_∞.

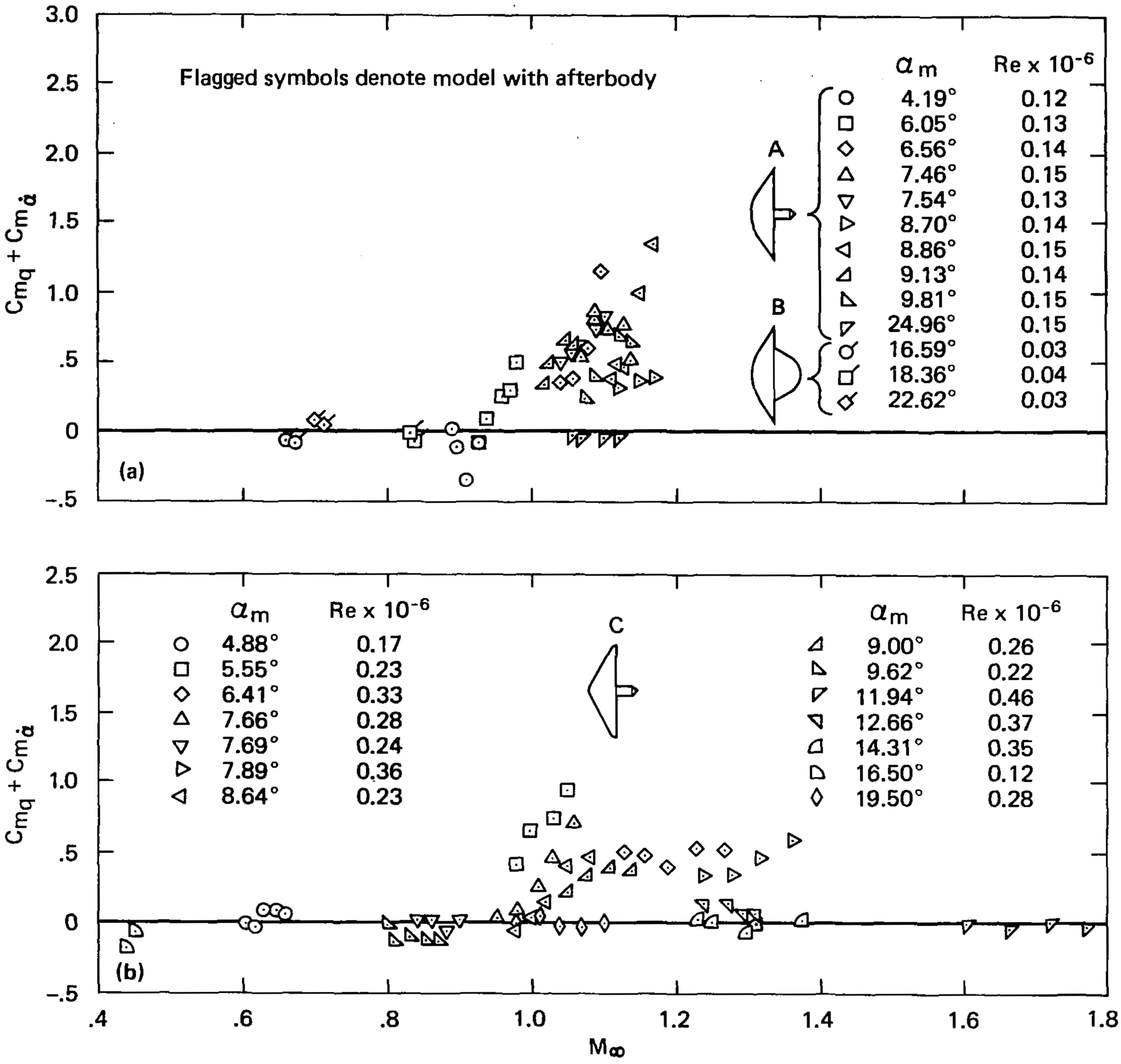

(a) Models A and B.
(b) Model C.

Figure 5.- Variation of the dynamic stability ($C_{m_q} + C_{m_{\dot\alpha}}$) with M_∞.

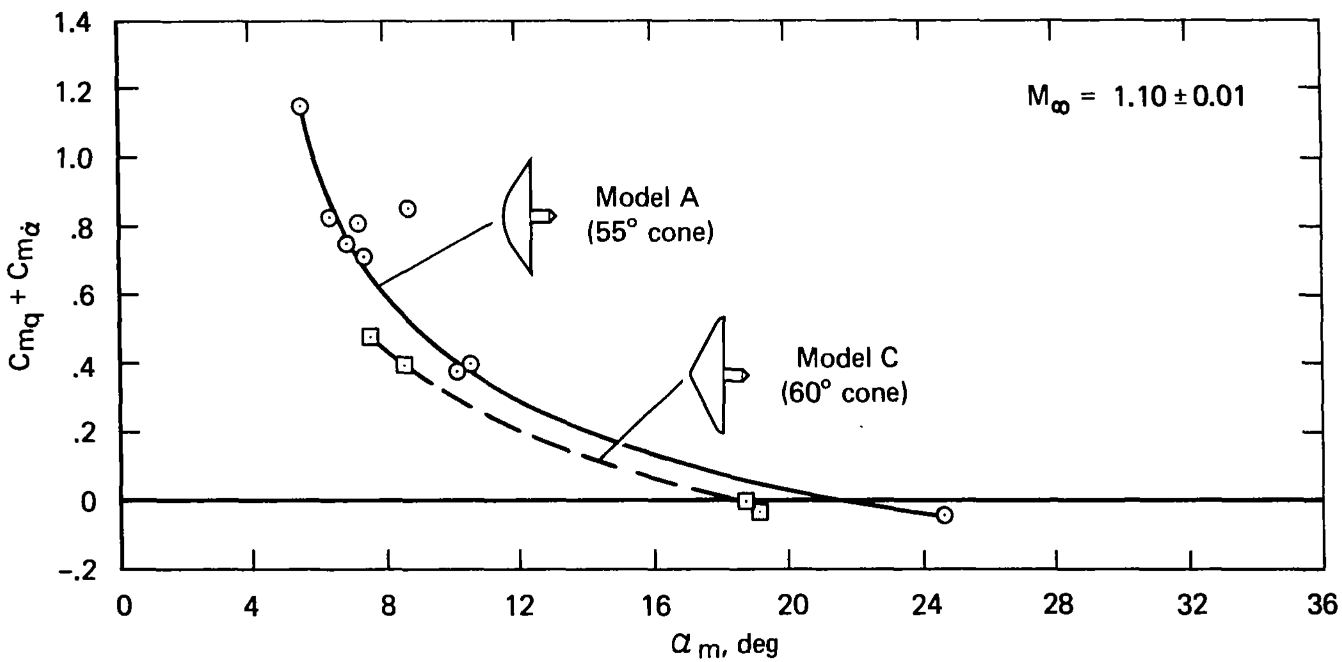

Figure 6.- Effect of pitch amplitude on the dynamic stability of models A and C.

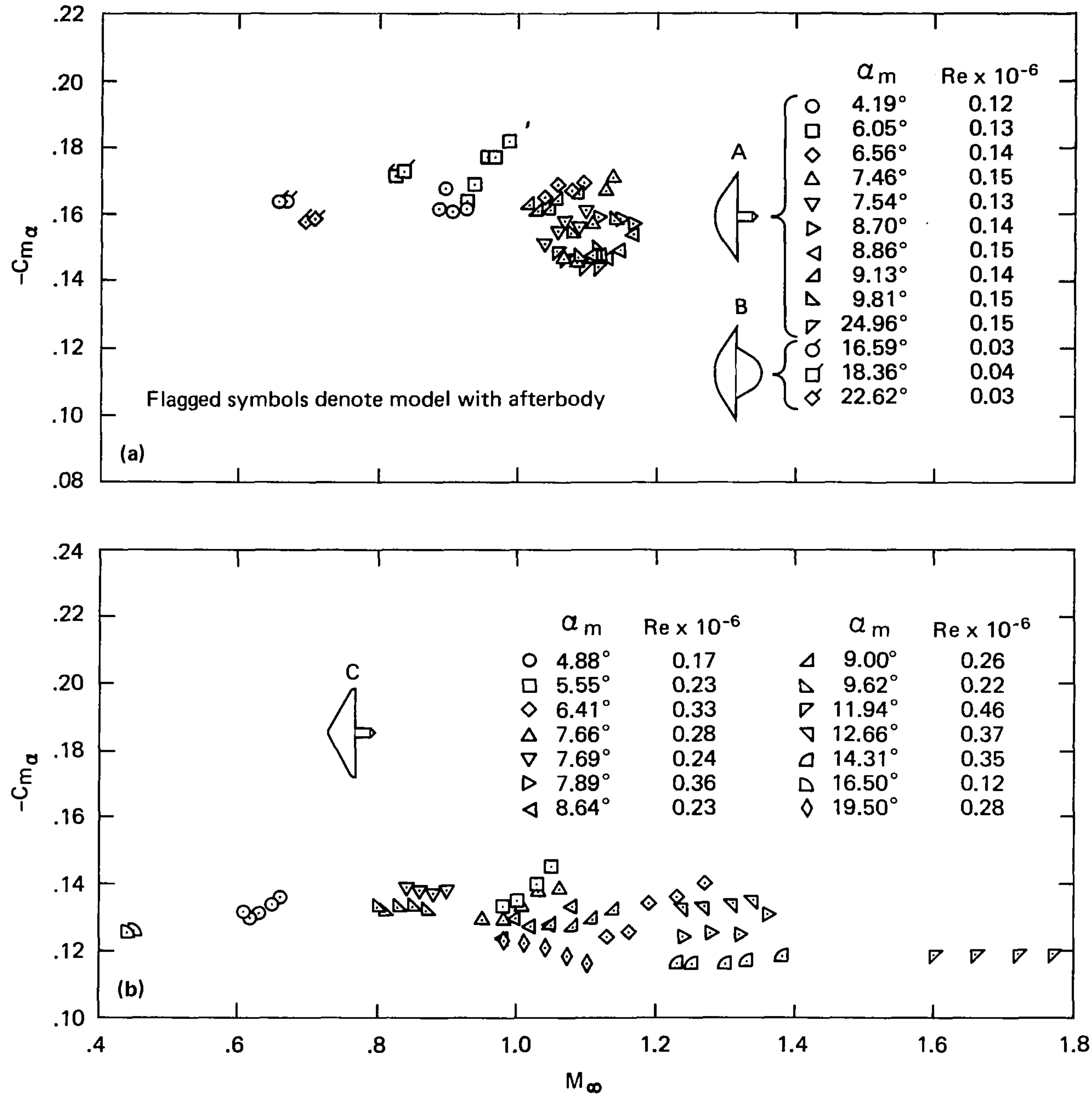

(a) Models A and B.
(b) Model C.

Figure 7.- Variation of the static stability derivative (C_{m_α}) with M_∞.

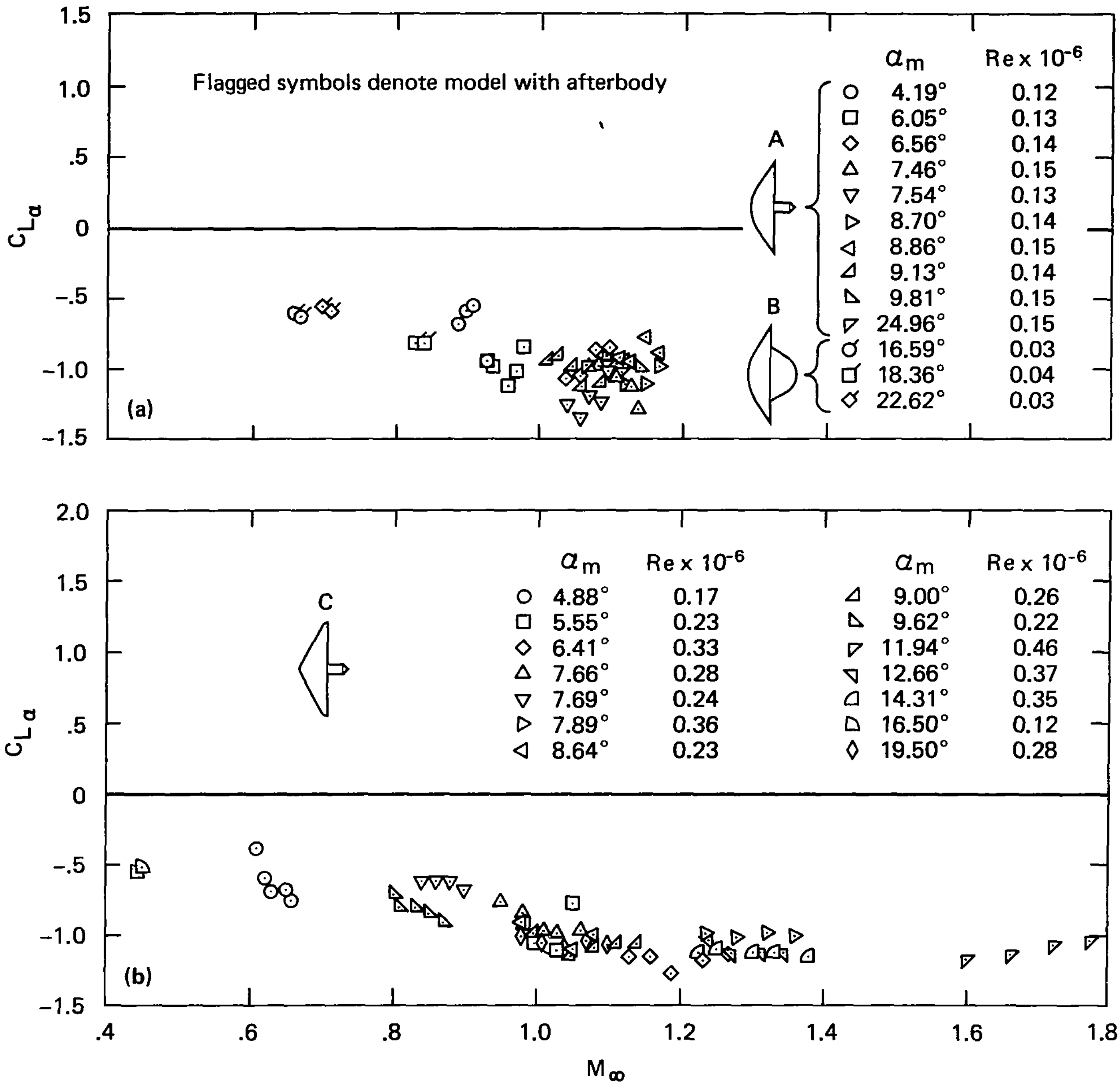

(a) Models A and B.
(b) Model C.

Figure 8.- Variation of the lift-curve slope (C_{L_α}) with M_∞.

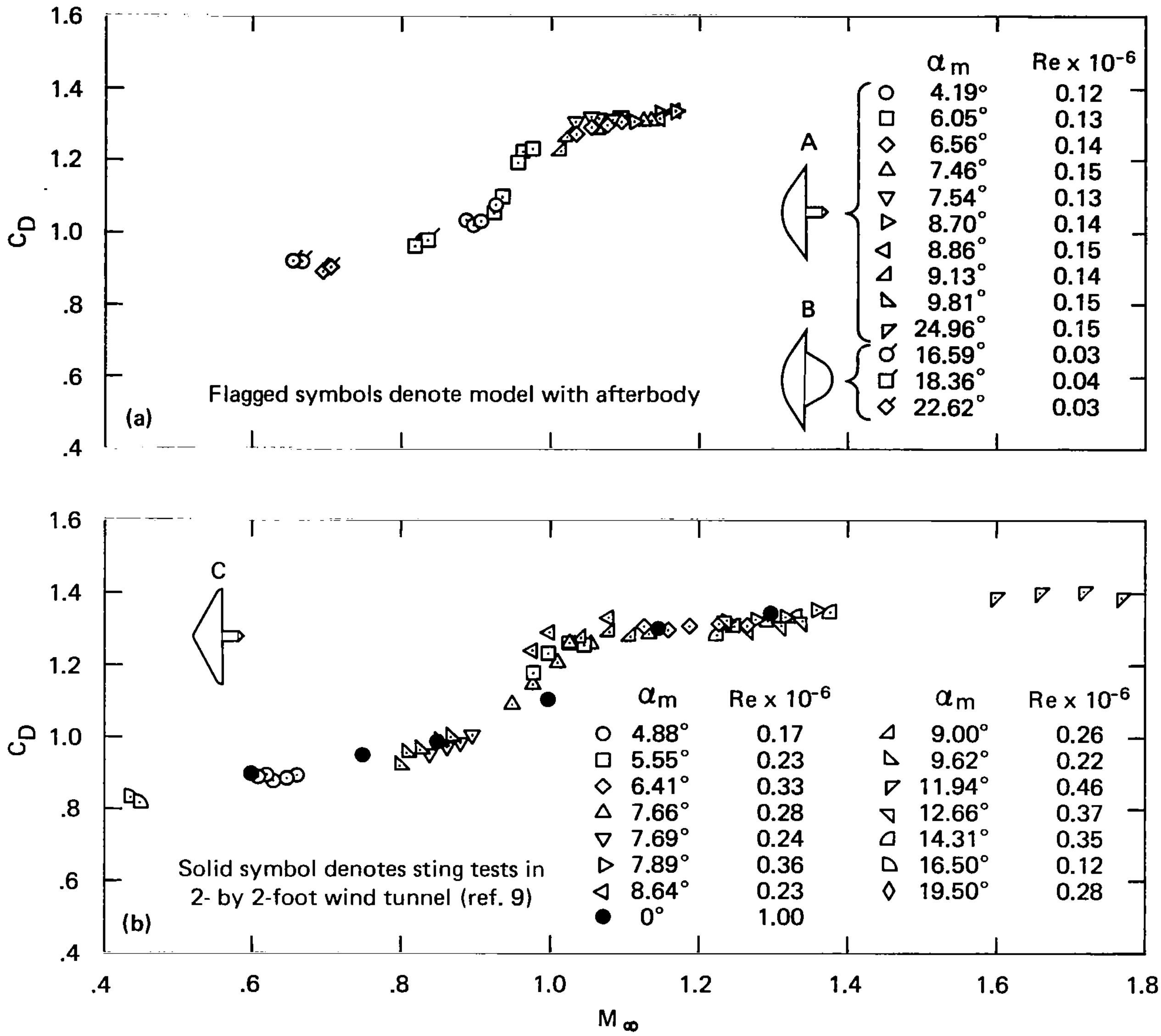

(a) Models A and B.
(b) Model C.

Figure 9.- Variation of the drag coefficient with M_∞.

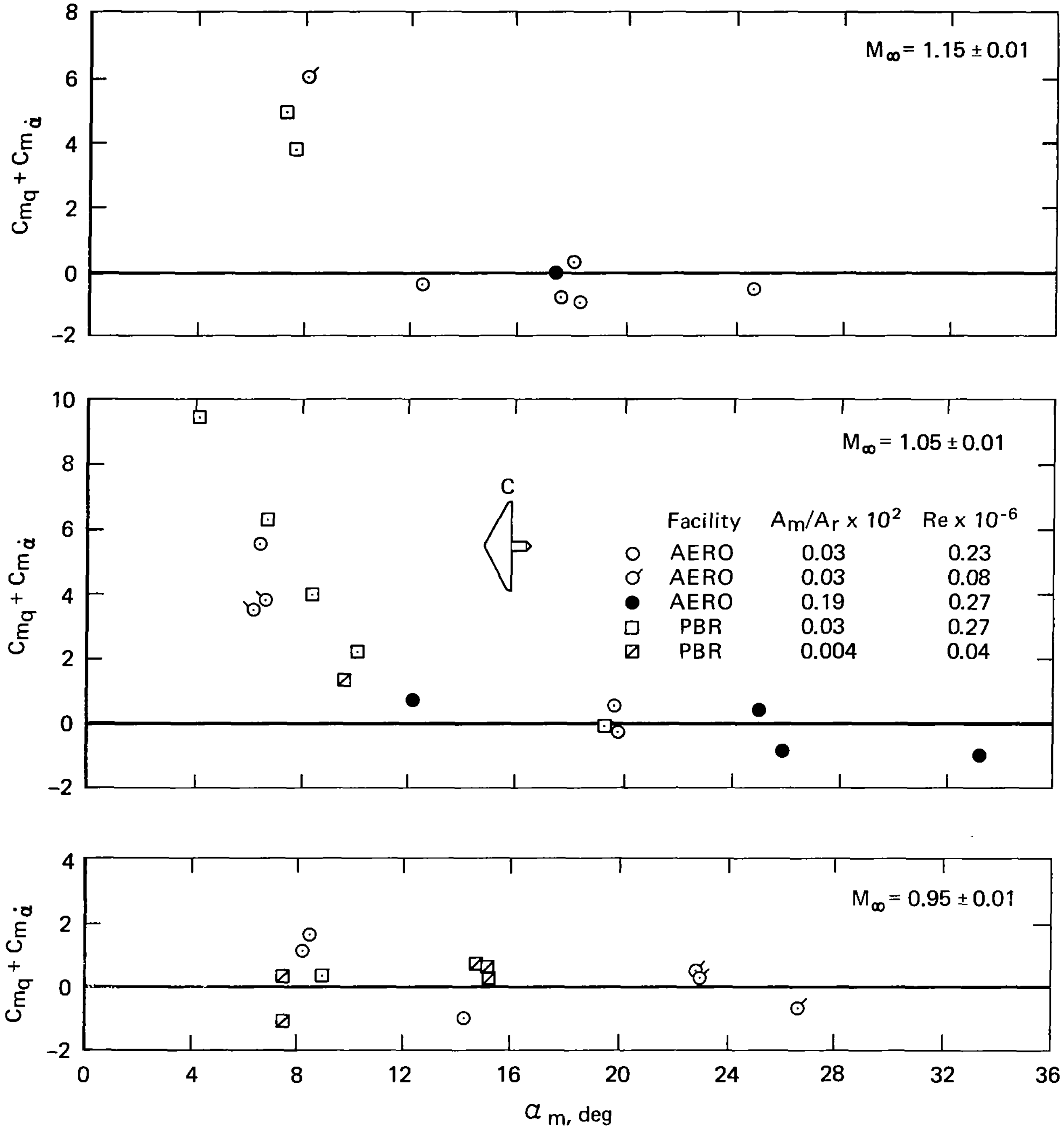

Figure 10.- Comparison of the dynamic stability of model C for three blockage factors in two facilities for nominal Mach numbers of 0.95, 1.05, and 1.15.

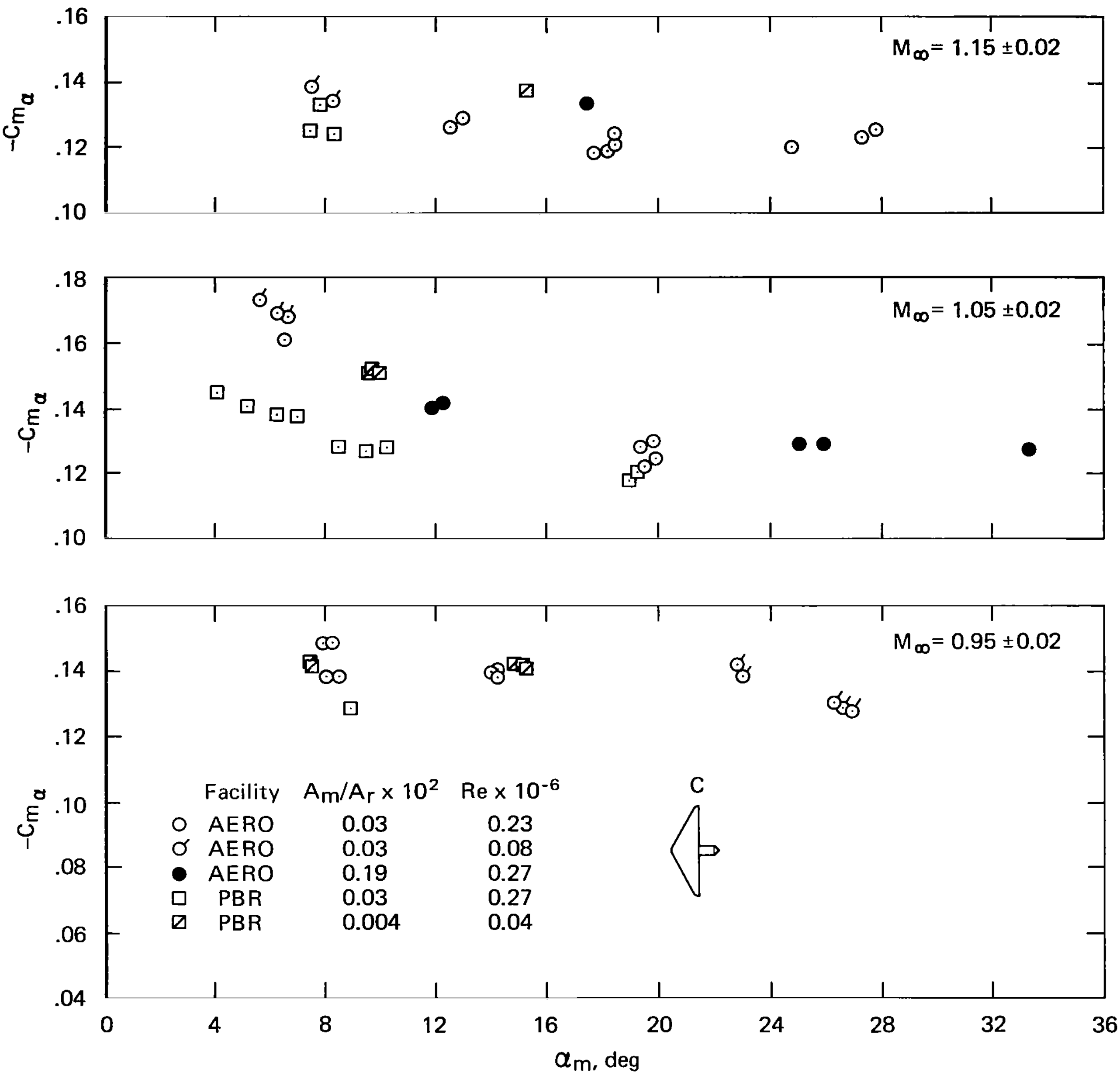

Figure 11.- Comparison of the static stability of model C for three blockage factors in two facilities for nominal Mach numbers of 0.95, 1.05, and 1.15.

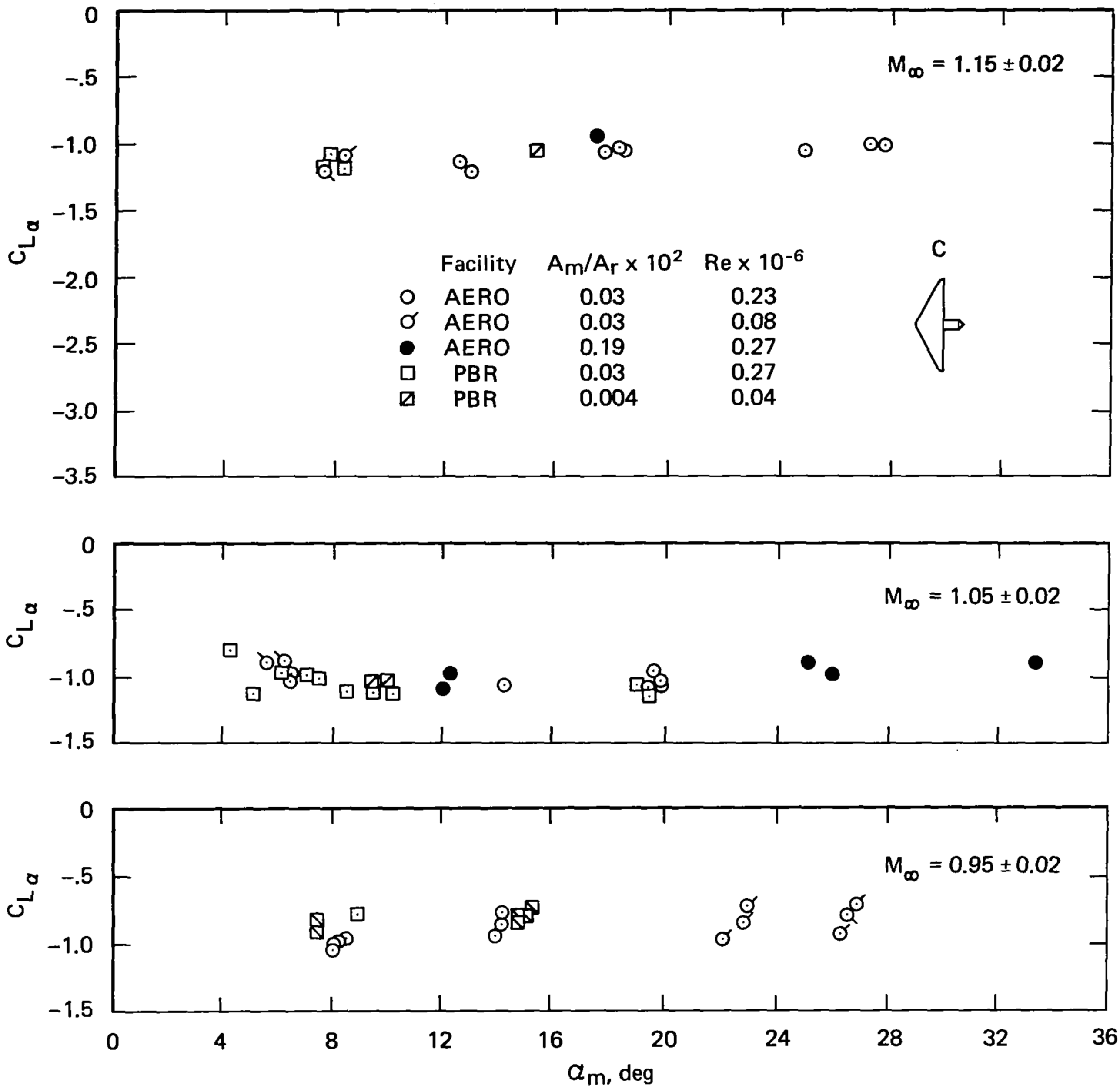

Figure 12.- Comparison of the lift-curve slope of model C for three blockage factors in two facilities for nominal Mach numbers of 0.95, 1.05, and 1.15.

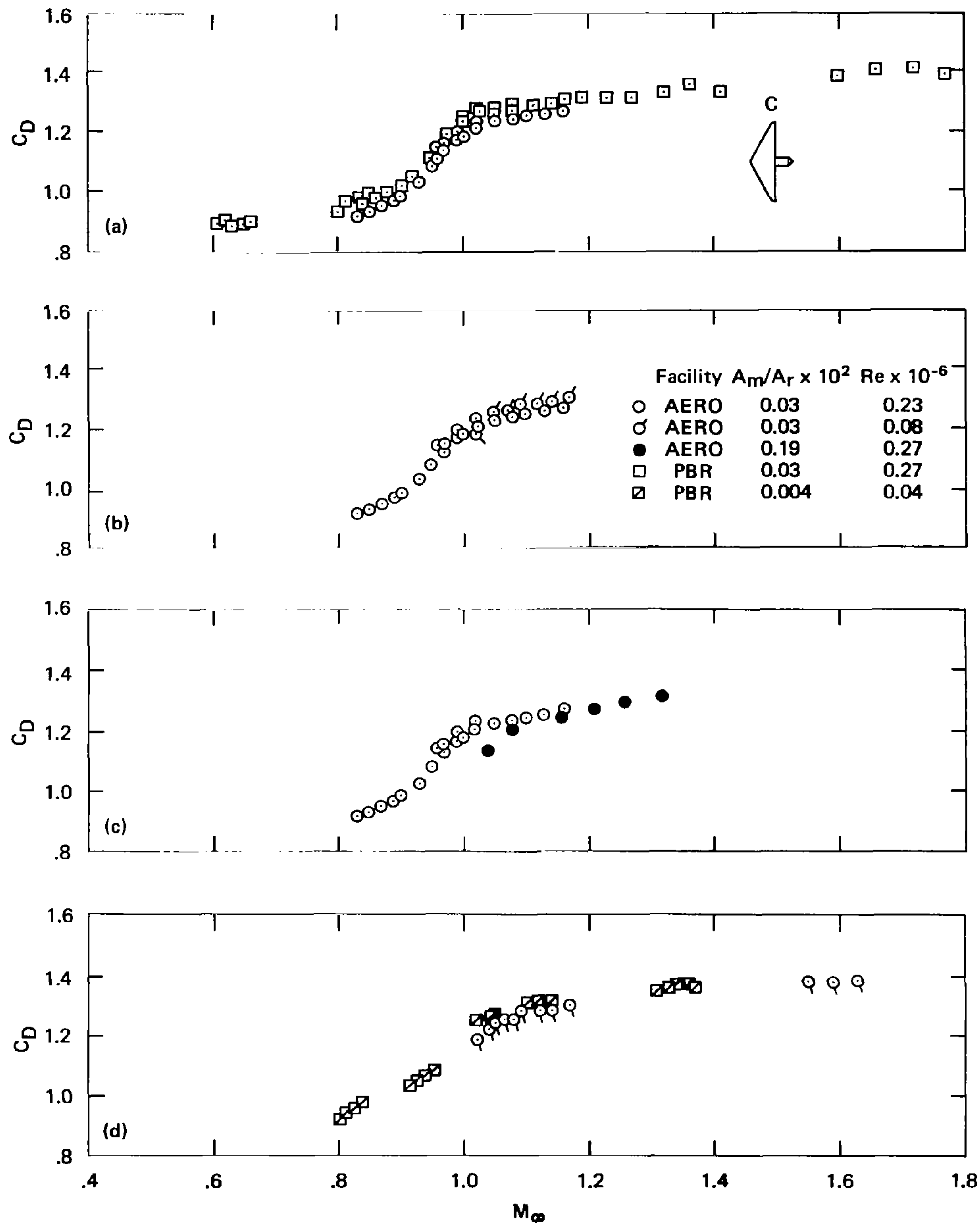

(a) Effect of facility.
(b) Effect of Reynolds number.
(c) Effect of blockage (high Re).
(d) Effect of blockage (low Re).

Figure 13.- Effect of facility, Reynolds number, and blockage on the drag coefficient of model C.

HYPERVELOCITY FREE–FLIGHT

AERODYNAMIC FACILITY

(AERO)

External
Electronics, Optics
and Fiducial System

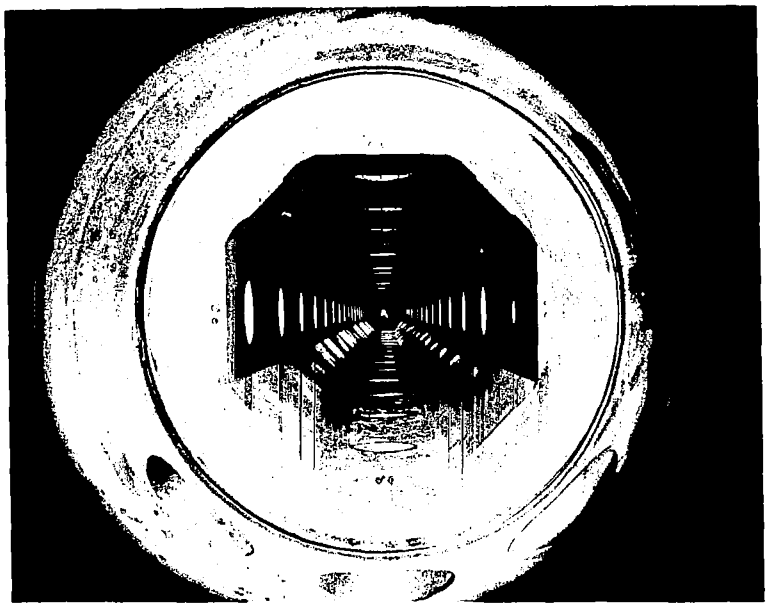

Distance Across Windows:
STA 1 = 1.30 m
STA 16 = 0.98 m
(Equiv Av Circular Dia = 1.18)

PRESSURIZED BALLISTIC

RANGE

(PBR)

Internal
Electronics, Optics
and Fiducial System

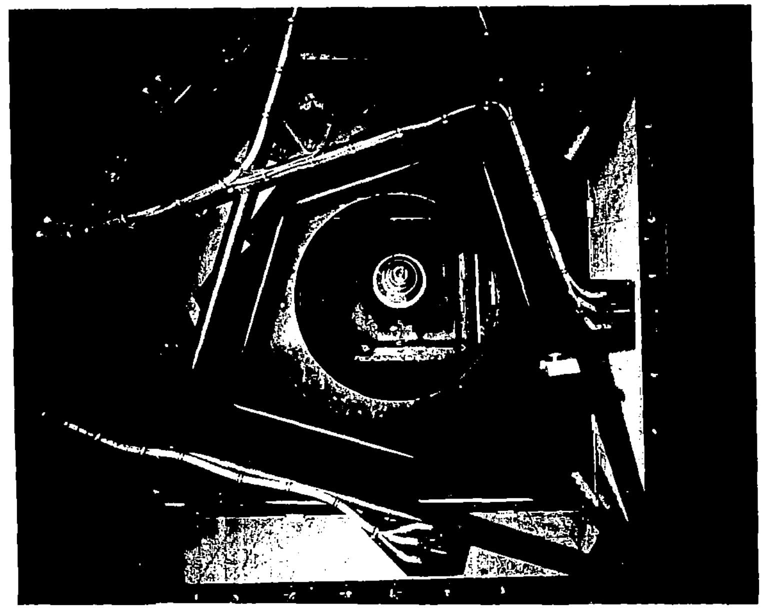

Centerline Distance to Film Plane:
STA 1 - 7 = 0.25 m
STA 8 - 17 = 0.50 m
STA 18 - 24 = 0.76 m
(Pressurized Shell Dia = 3.04 m)

(Model Diameters = 0.02 - 0.05 m)

Figure 14.- Facility internal geometry.

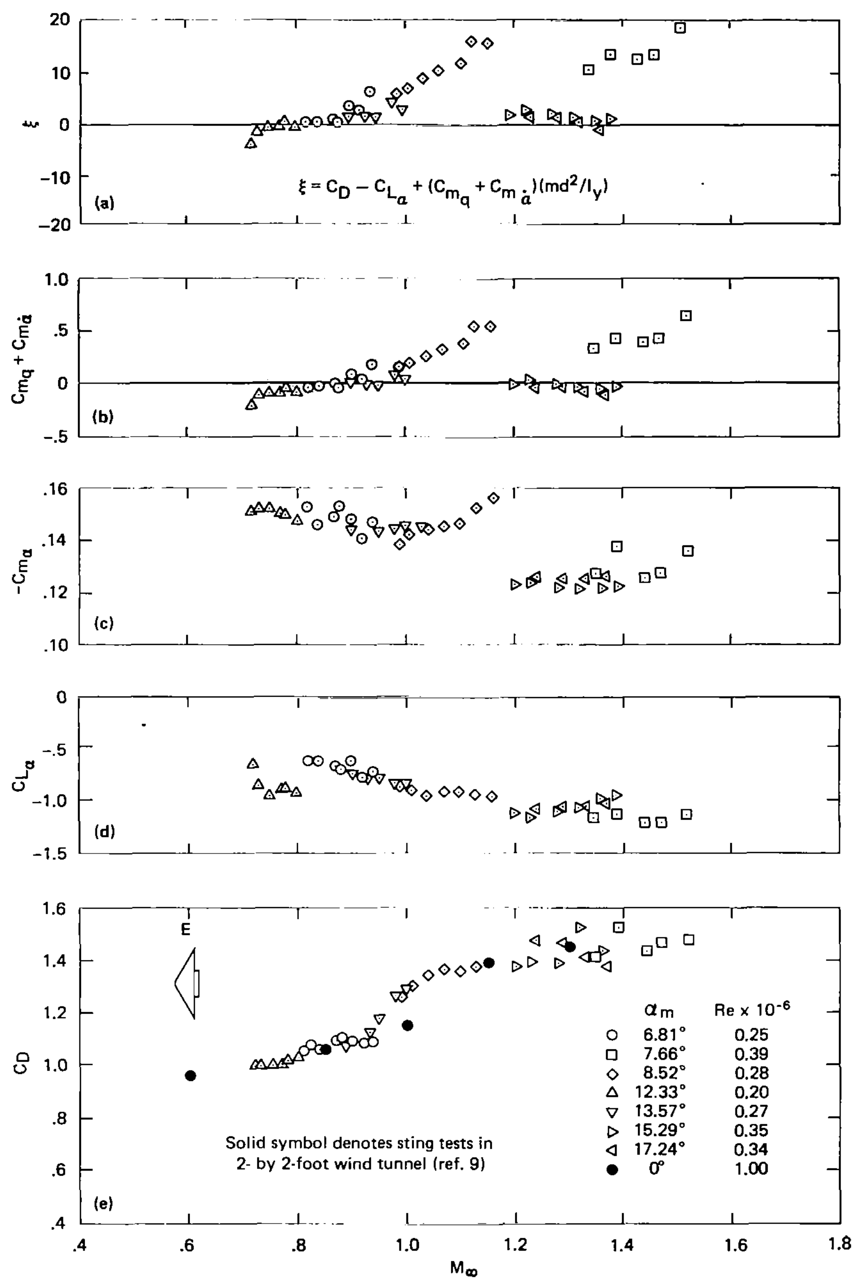

(a) Damping parameter, ξ

(b) Dynamic stability, $C_{m_q} + C_{m_{\dot{\alpha}}}$

(c) Static stability, C_{m_α}

(d) Lift-curve slope, C_{L_α}

(e) Drag

Figure 15.- Aerodynamic characteristics of model E (d = 5.08 cm) in P.B.R.

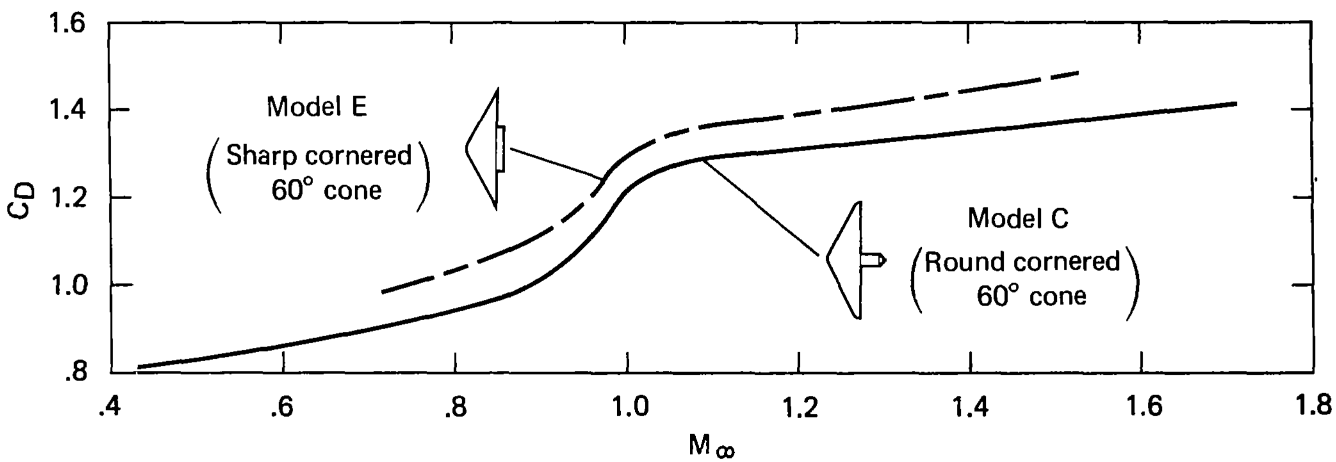

Figure 16.- Comparison of the drag coefficients obtained for models C and E.

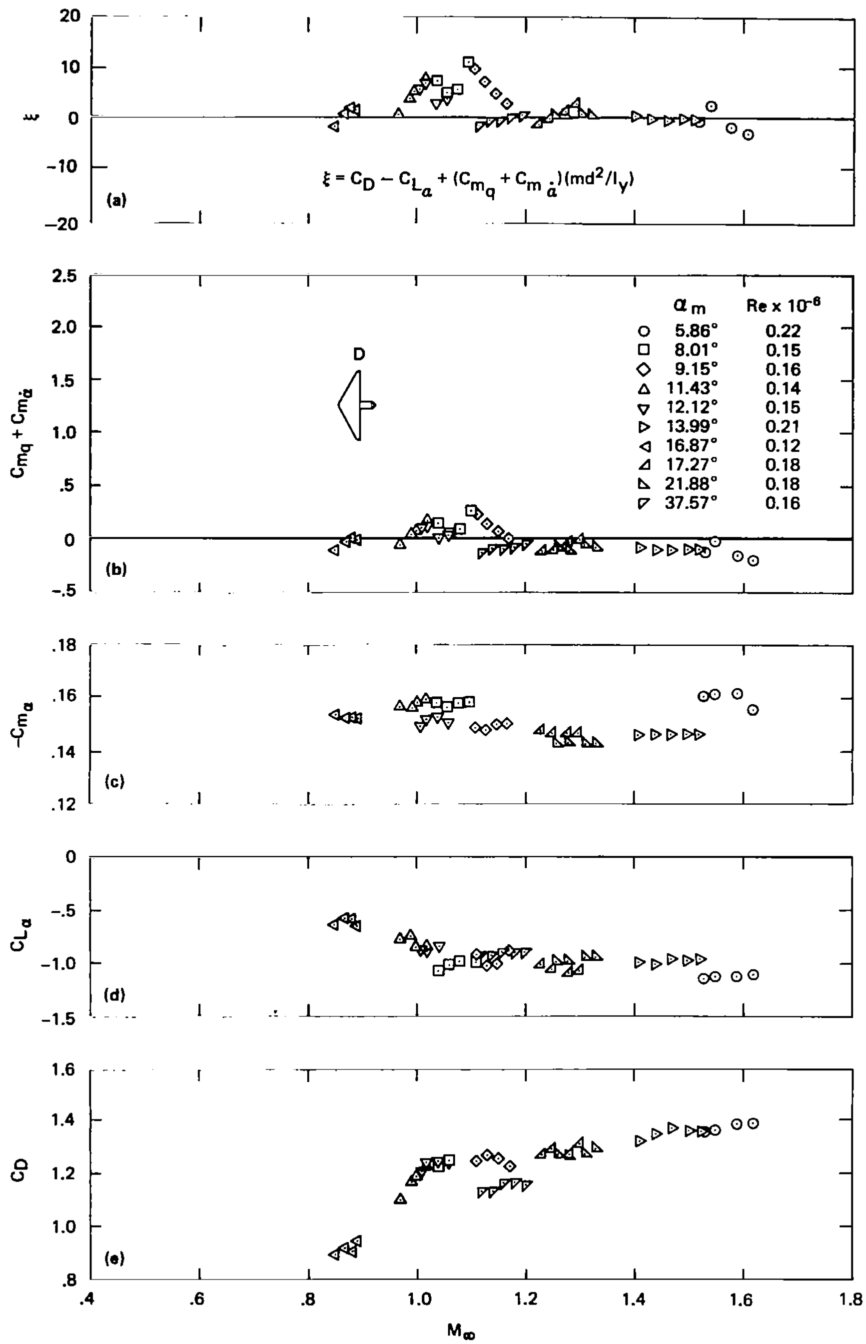

(a) Damping parameter, ξ

(b) Dynamic stability, $C_{m_q} + C_{m_{\dot\alpha}}$

(c) Static stability, C_{m_α}

(d) Lift-curve slope, C_{L_α}

(e) Drag

Figure 17.- Aerodynamic characteristics of model D ($x_{cg}/d = 0.17$) in the P.B.R.

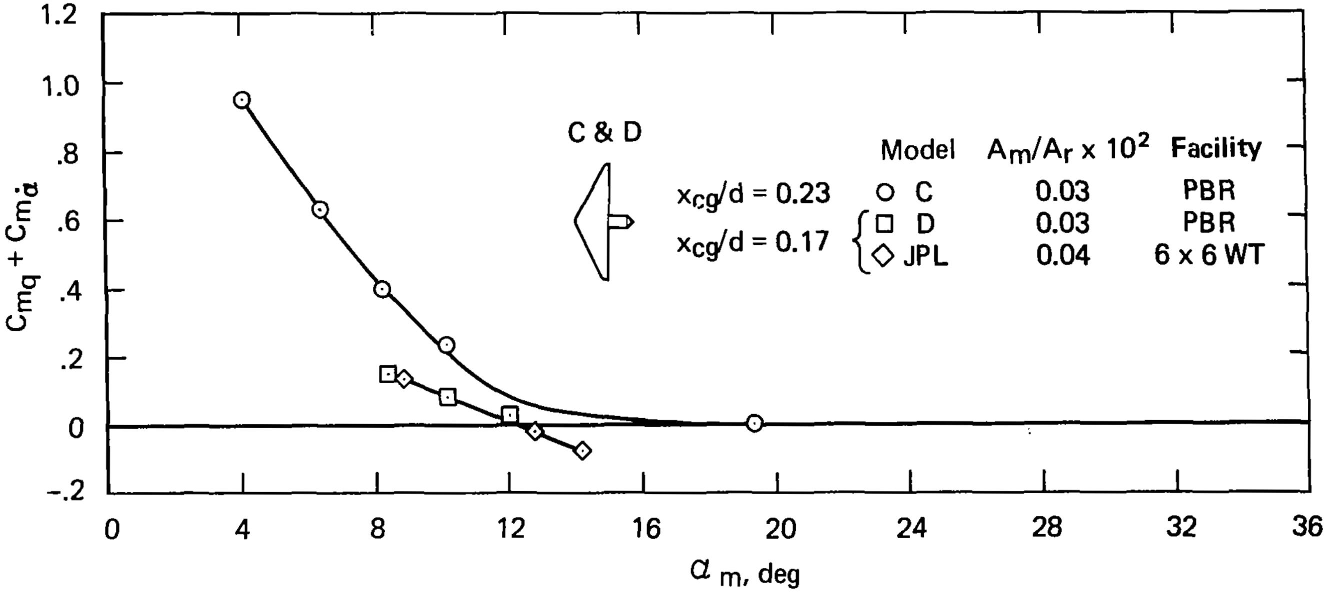

Figure 18.- The effect of center-of-gravity location on the dynamic stability of the 60° half-angle blunted cone at a Mach number of 1.05.

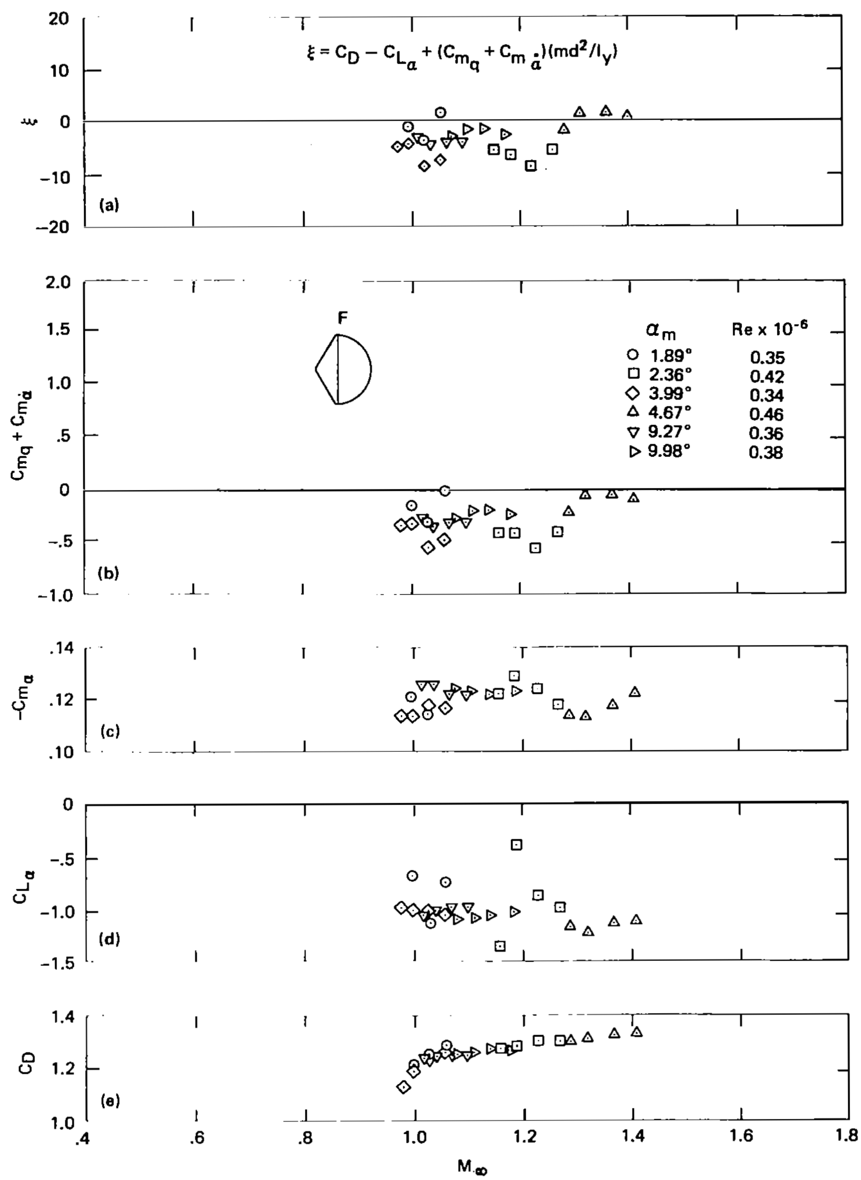

(a) Damping parameter

(b) Dynamic stability, $C_{m_q} + C_{m_{\dot\alpha}}$

(c) Static stability, C_{m_α}

(d) Lift-curve slope, C_{L_α}

(e) Drag

Figure 19.- Aerodynamic characteristics of the 60° half-angle blunted cone with a spherical afterbody, model F.

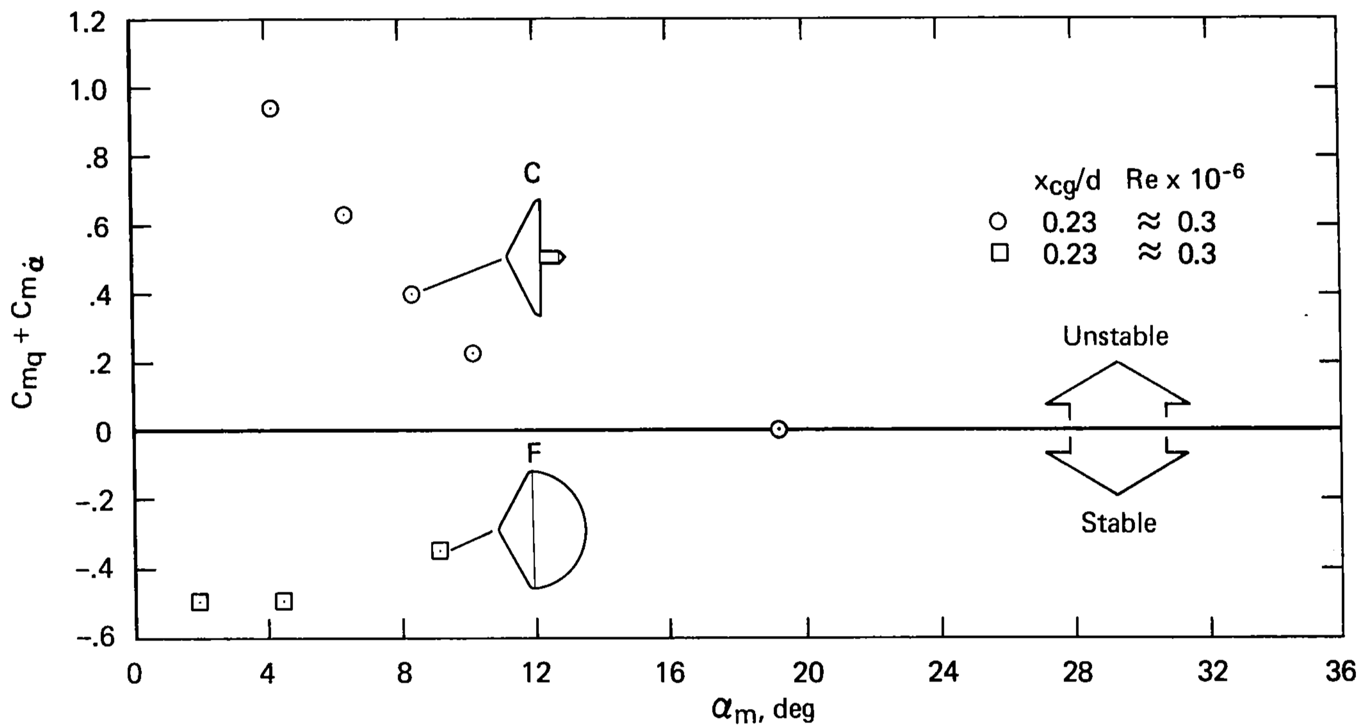

Figure 20.- Effect of afterbody shape on the dynamic stability ($C_{m_q} + C_{m_{\dot{\alpha}}}$) of a 60° half-angle cone at a Mach number of 1.05.

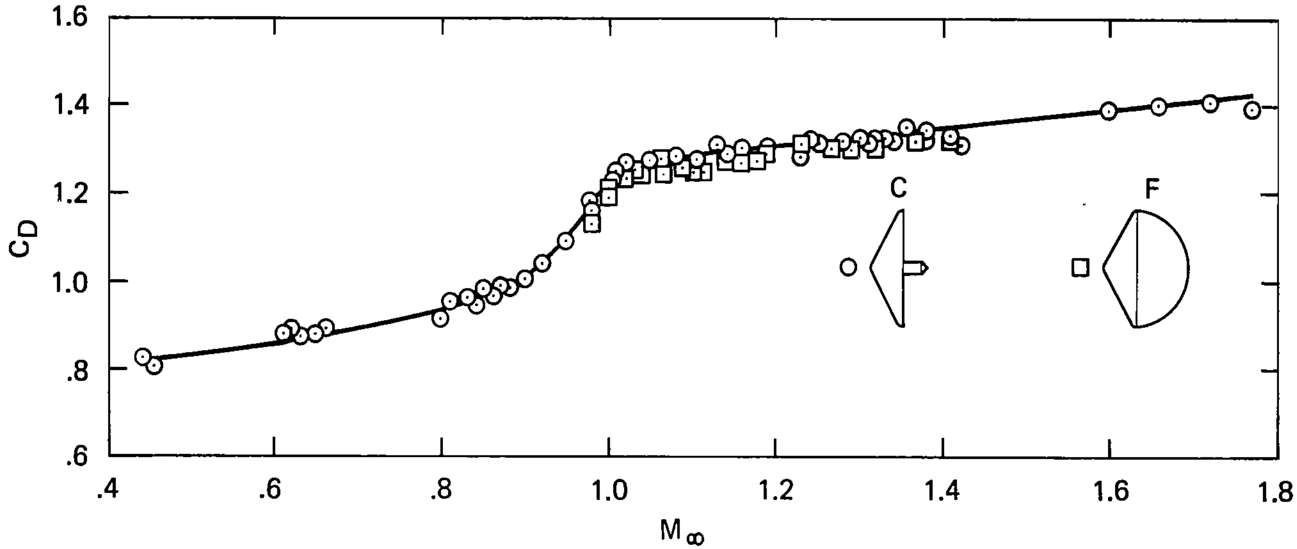

Figure 21.- The effect of afterbody shape on the drag coefficient of the 60° half-angle blunted cone.

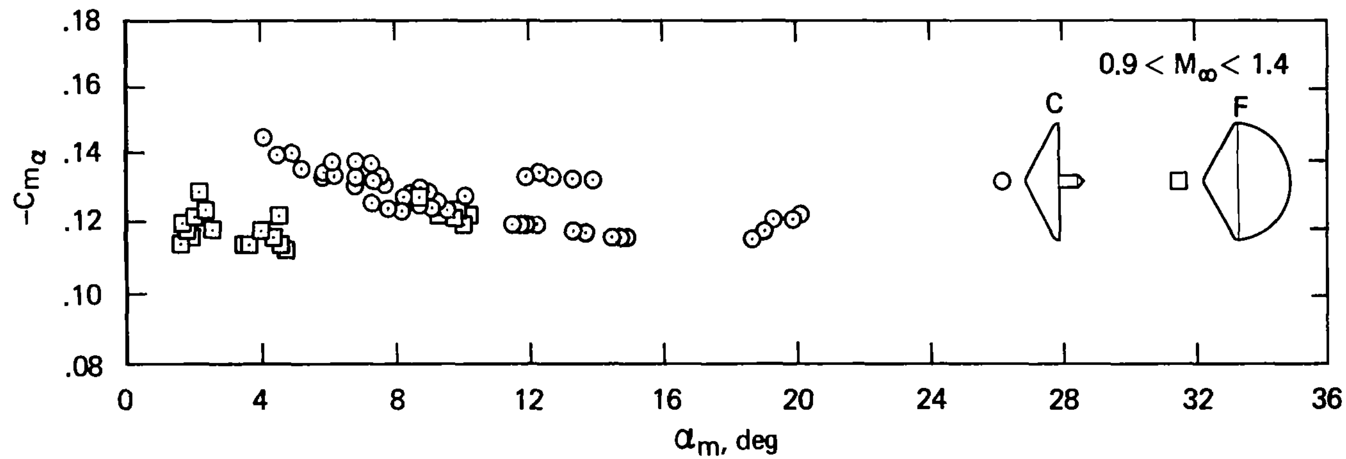

Figure 22.- Effect of afterbody shape on the static stability of the 60° half-angle blunted cone.

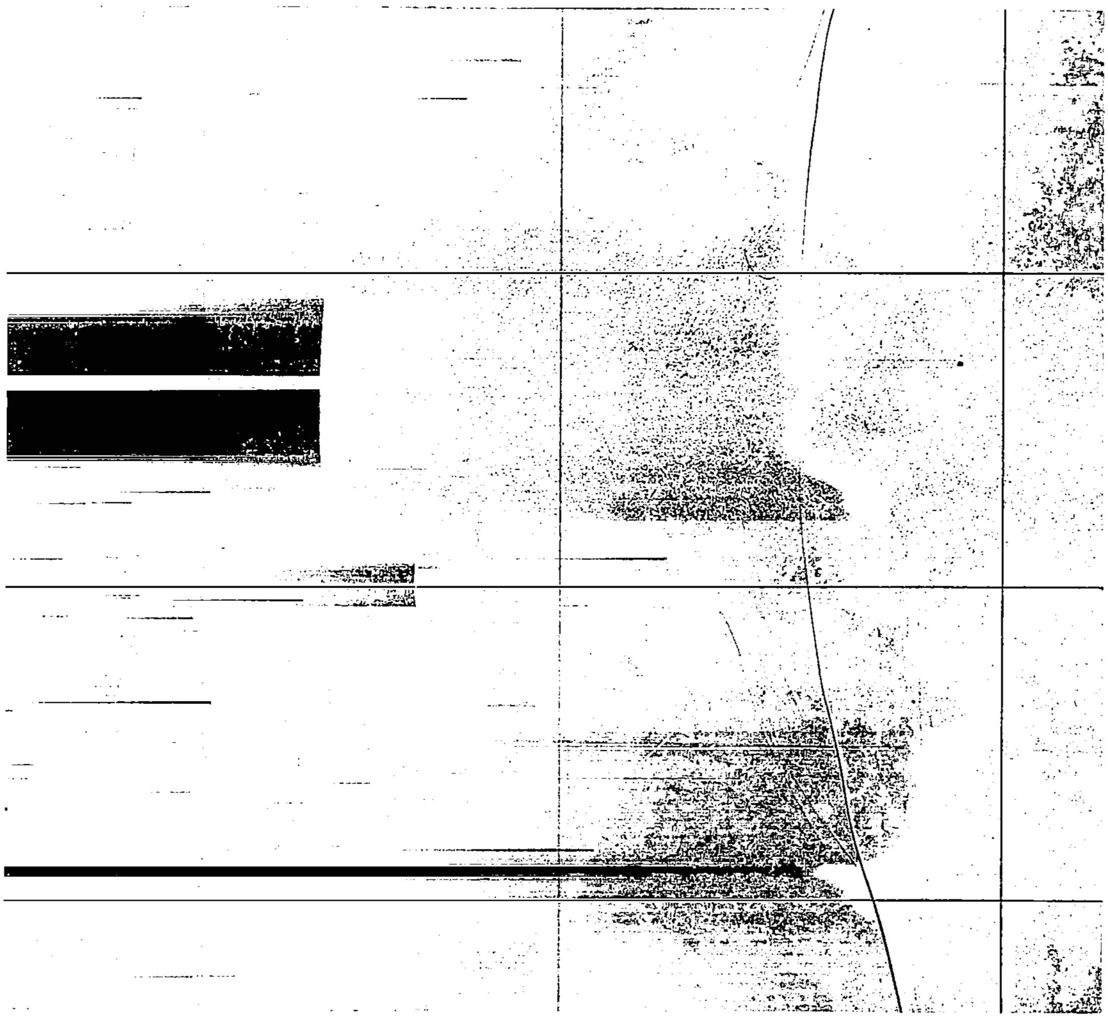

(a) Model C, $M_\infty \approx 0.994$, $\alpha = 1.02°$.

Figure 23.- Wake details.

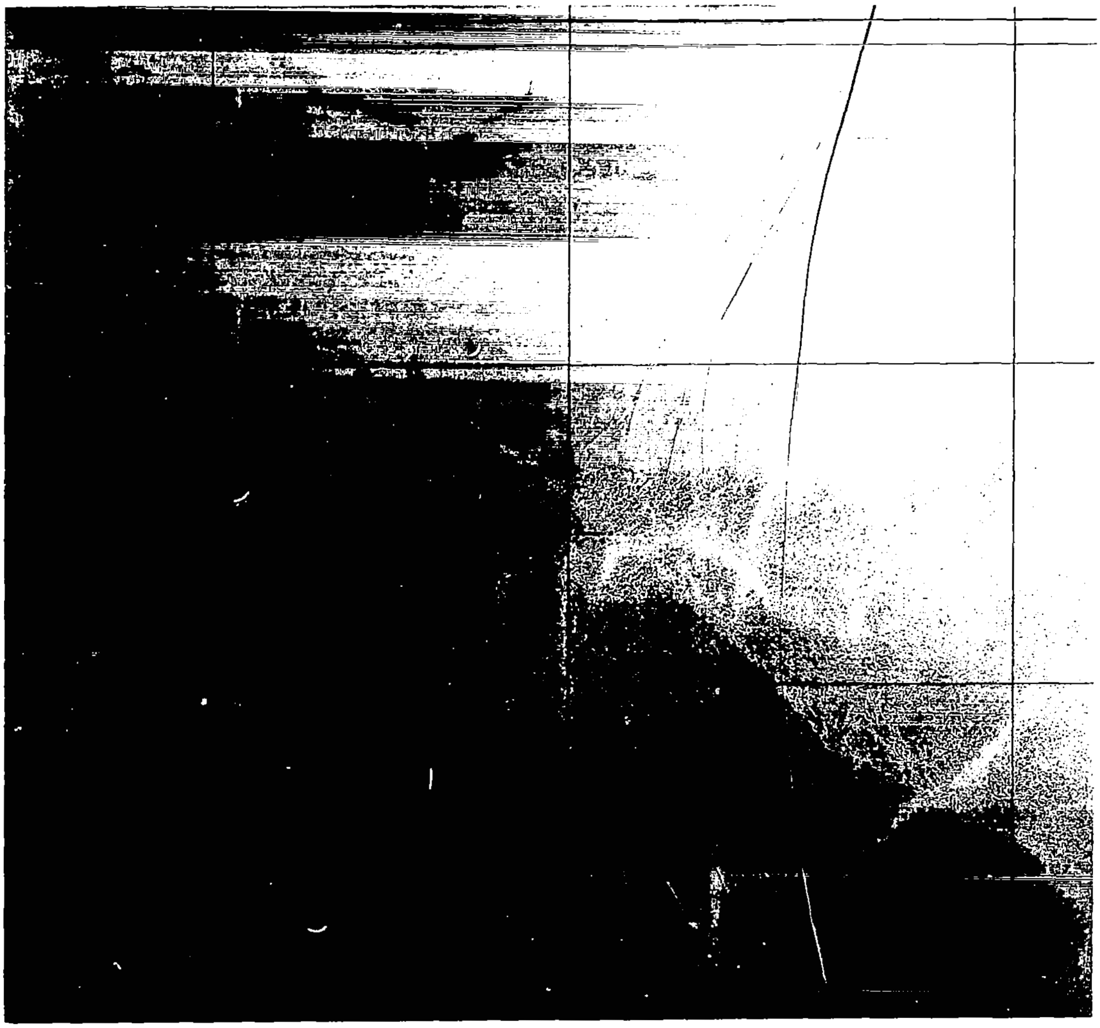

(b) Model F, $M_\infty \approx 0.996$, $\alpha = 1.22°$.

Figure 23.- Continued.

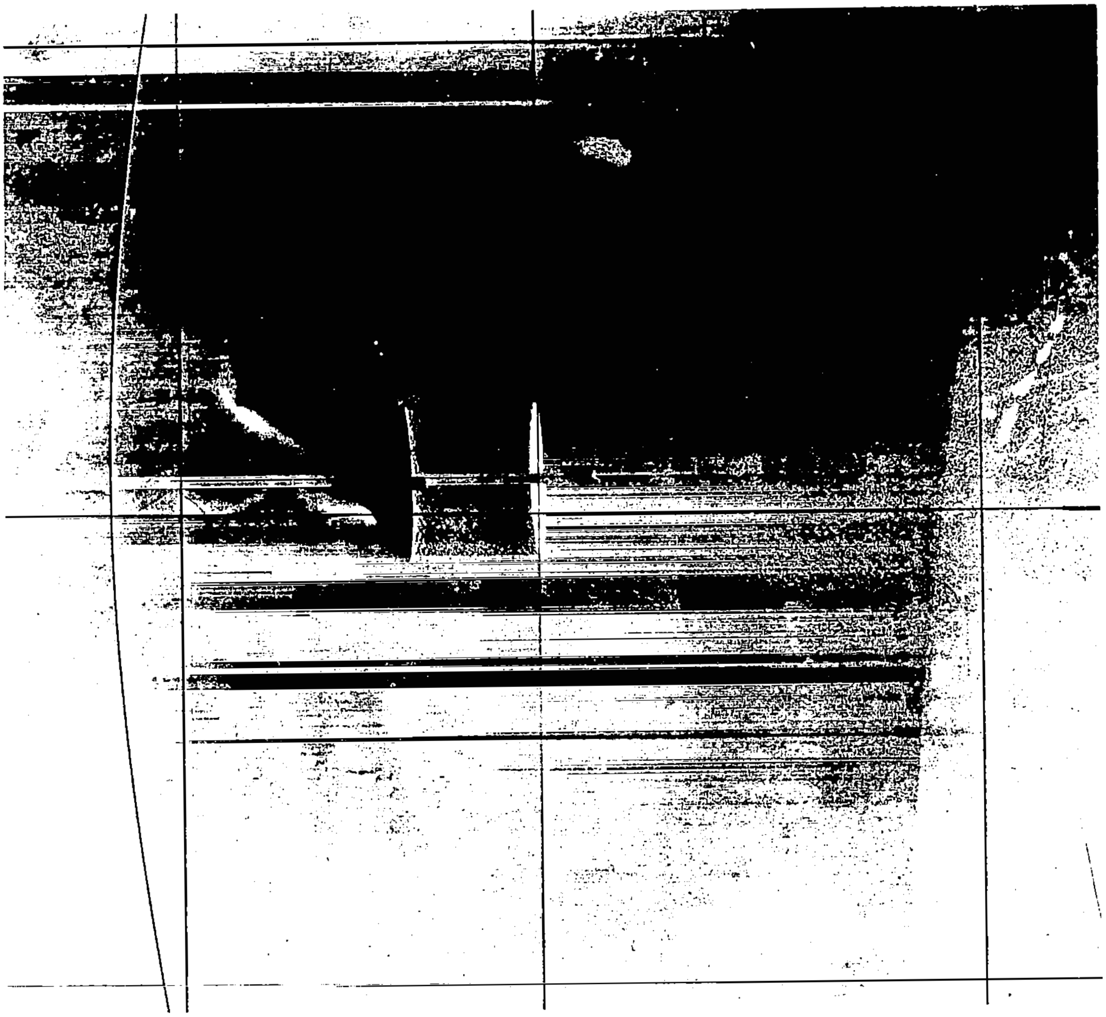

(c) Model C, $M_\infty \approx 1.08$, $\alpha = 1.53°$.

Figure 23.- Continued.

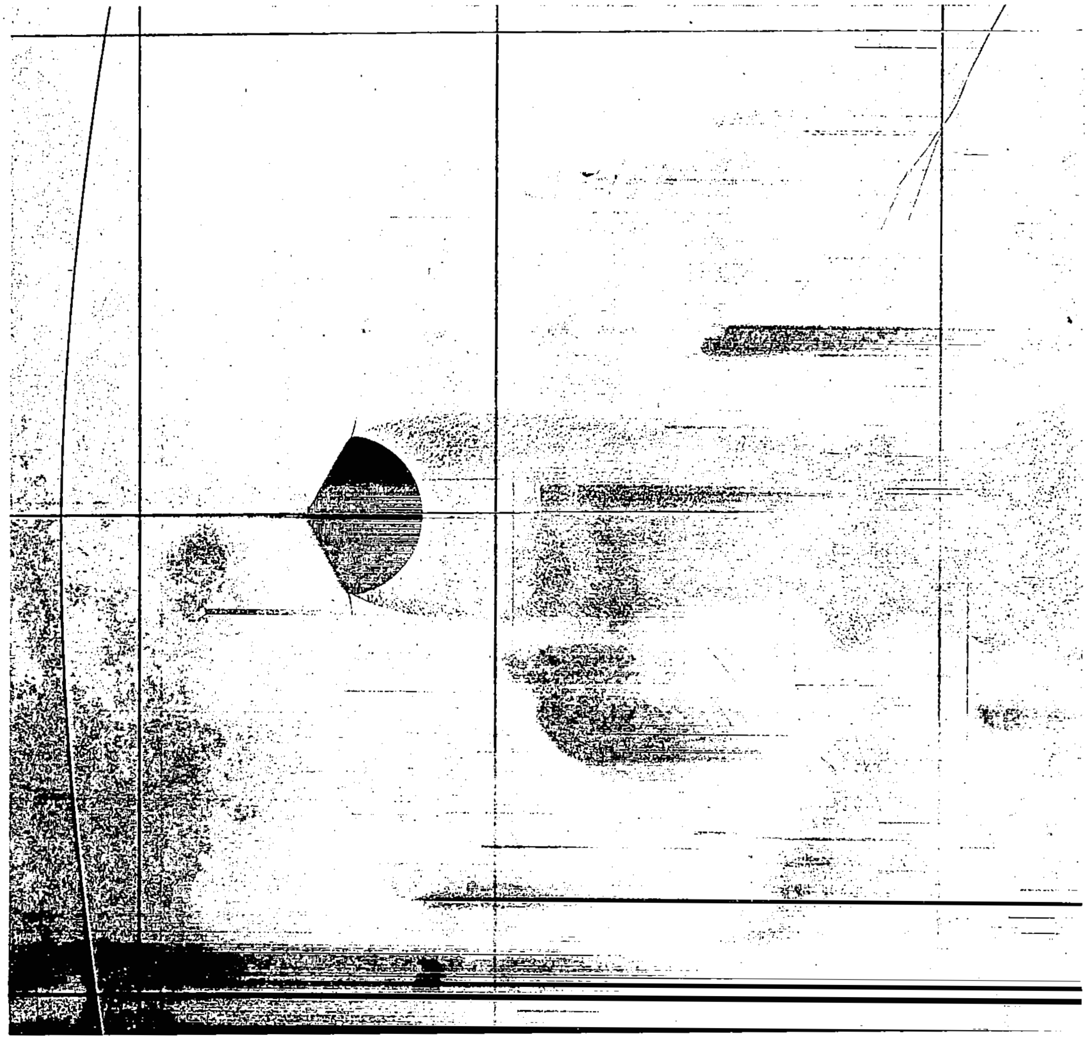

(d) Model F, $M_\infty \approx 1.08$, $\alpha = 0.32°$.

Figure 23.- Concluded.

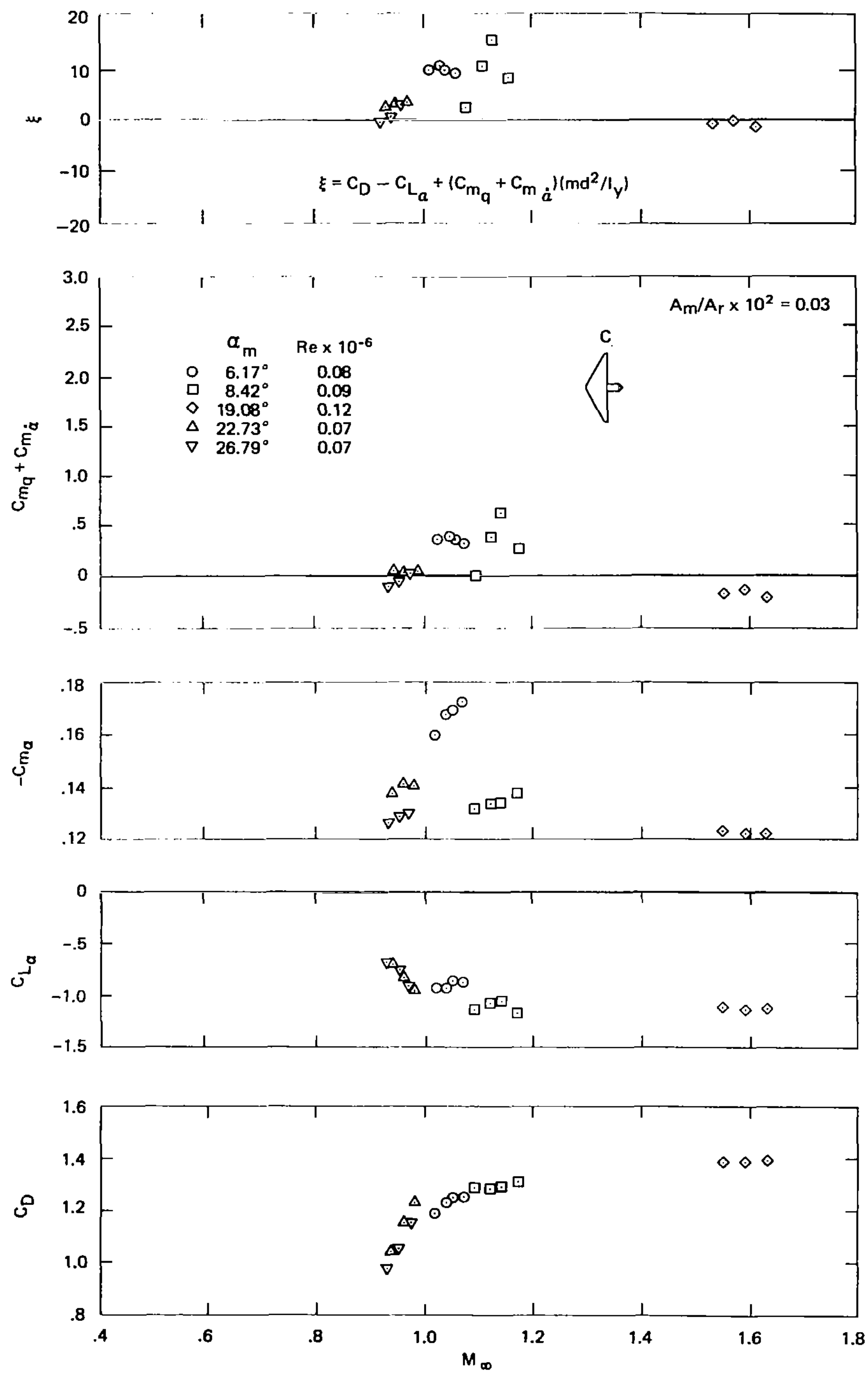

(a) Low Reynolds number ($0.07 \times 10^6 < Re < 0.12 \times 10^6$).

Figure 24.- Aerodynamic characteristics of model C (d = 2.03 cm) in Aero facility.

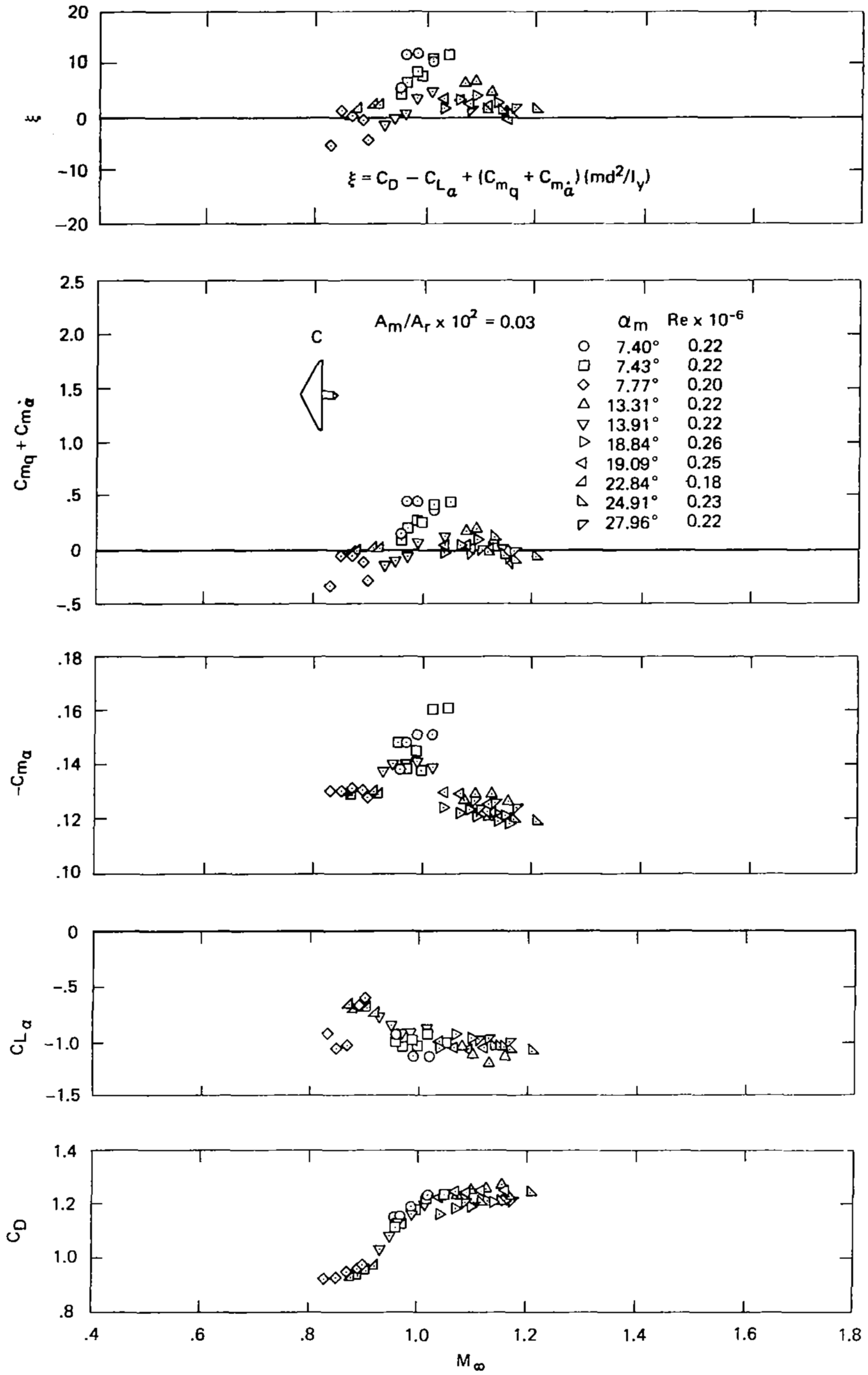

(b) High Reynolds number ($0.18 \times 10^6 < Re < 0.26 \times 10^6$).

Figure 24.- Concluded.

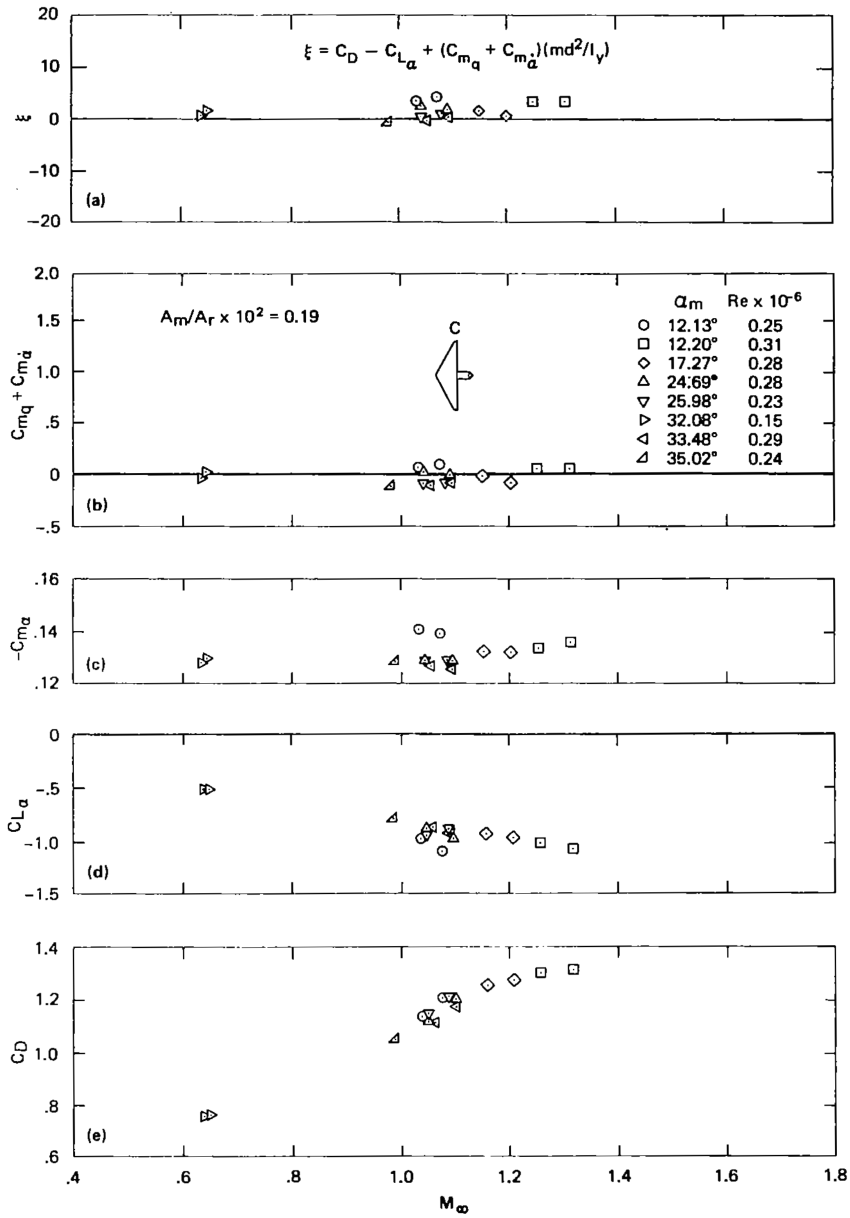

(a) Damping parameter, ξ
(b) Dynamic stability, $C_{m_q} + C_{m_{\dot\alpha}}$
(c) Static stability, C_{m_α}
(d) Lift-curve slope, C_{L_α}
(e) Drag

Figure 25.- Aerodynamic characteristics of model C (d = 5.08 cm) in Aero facility.

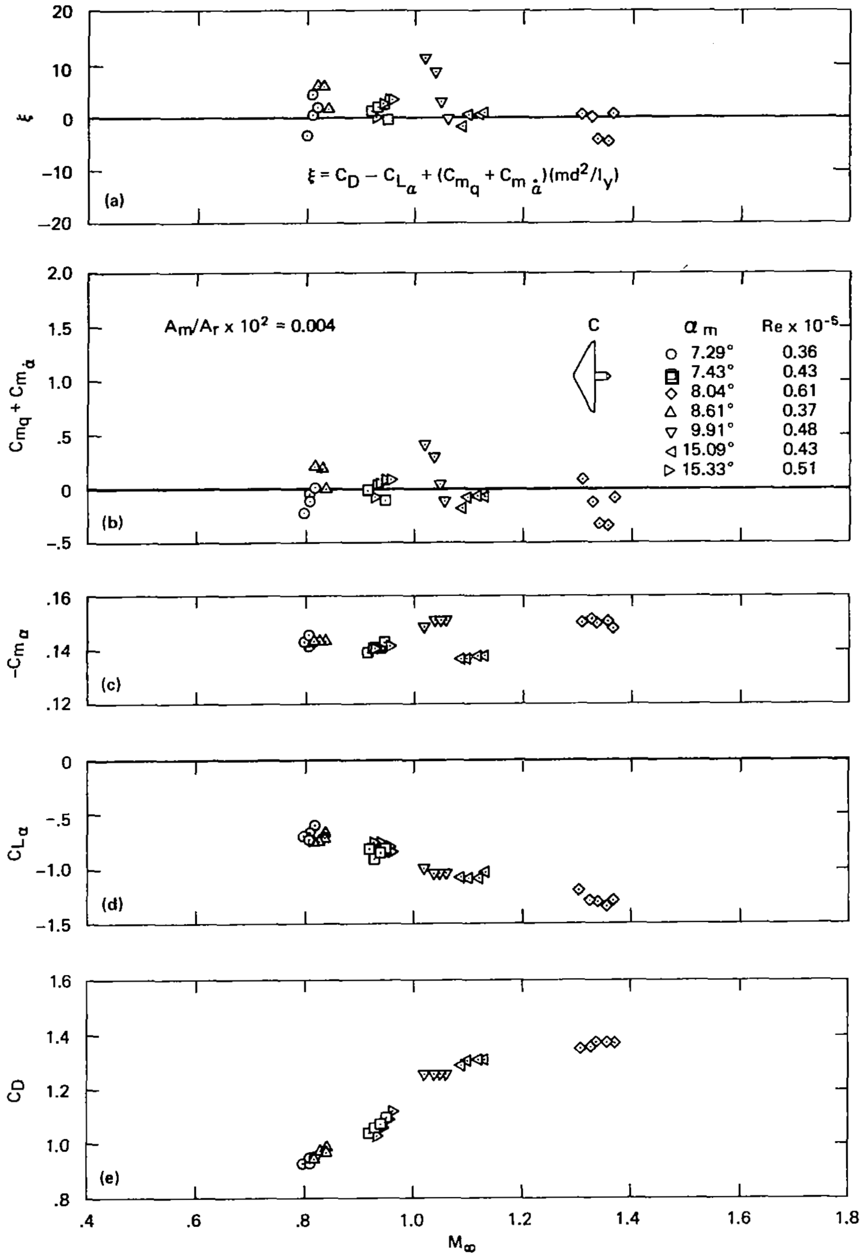

(a) Damping parameter, ξ
(b) Dynamic stability, $C_{m_q} + C_{m_{\dot{\alpha}}}$
(c) Static stability, C_{m_α}
(d) Lift-curve slope, C_{L_α}
(e) Drag

Figure 26.- Aerodynamic characteristics of model C (d = 2.03 cm) in P.B.R.

NASA-Langley, 1971 —— 1 A-3613

NATIONAL AERONAUTICS AND SPACE ADMINISTRATION
WASHINGTON, D.C. 20546

OFFICIAL BUSINESS
PENALTY FOR PRIVATE USE $300

FIRST CLASS MAIL

POSTAGE AND FEES PAID
NATIONAL AERONAUTICS AN
SPACE ADMINISTRATION

015 001 C1 U 01 710820 S00903DS
DEPT OF THE AIR FORCE
AF SYSTEMS COMMAND
AF WEAPONS LAB (WLOL)
ATTN: E LOU BOWMAN, CHIEF TECH LIBRARY
KIRTLAND AFB NM 87117

POSTMASTER: If Undeliverable (Section 158 Postal Manual) Do Not Retur

---

"The aeronautical and space activities of the United States shall be conducted so as to contribute . . . to the expansion of human knowledge of phenomena in the atmosphere and space. The Administration shall provide for the widest practicable and appropriate dissemination of information concerning its activities and the results thereof."

—NATIONAL AERONAUTICS AND SPACE ACT OF 1958

NASA SCIENTIFIC AND TECHNICAL PUBLICATIONS

TECHNICAL REPORTS: Scientific and technical information considered important, complete, and a lasting contribution to existing knowledge.

TECHNICAL NOTES: Information less broad in scope but nevertheless of importance as a contribution to existing knowledge.

TECHNICAL MEMORANDUMS: Information receiving limited distribution because of preliminary data, security classification, or other reasons.

CONTRACTOR REPORTS: Scientific and technical information generated under a NASA contract or grant and considered an important contribution to existing knowledge.

TECHNICAL TRANSLATIONS: Information published in a foreign language considered to merit NASA distribution in English.

SPECIAL PUBLICATIONS: Information derived from or of value to NASA activities. Publications include conference proceedings, monographs, data compilations, handbooks, sourcebooks, and special bibliographies.

TECHNOLOGY UTILIZATION PUBLICATIONS: Information on technology used by NASA that may be of particular interest in commercial and other non-aerospace applications. Publications include Tech Briefs, Technology Utilization Reports and Technology Surveys.

Details on the availability of these publications may be obtained from:

SCIENTIFIC AND TECHNICAL INFORMATION OFFICE

NATIONAL AERONAUTICS AND SPACE ADMINISTRATION

Washington, D.C. 20546